

# Generalized Simultaneous Component Analysis of Binary and Quantitative data

Yipeng Song<sup>1</sup>, Johan A. Westerhuis<sup>1</sup>, Nanne Aben<sup>2</sup>, Lodewyk F.A. Wessels<sup>2</sup>,  
Patrick J.F. Groenen<sup>3</sup> and Age K. Smilde<sup>1</sup>

<sup>1</sup>Swammerdam Institute for Life Sciences, University of Amsterdam

<sup>2</sup>Division of Molecular Carcinogenesis, The Netherlands Cancer Institute

<sup>3</sup>Econometric Institute, Erasmus School of Economics, Erasmus University

## Abstract

In the current era of systems biological research there is a need for the integrative analysis of binary and quantitative genomics data sets measured on the same objects. We generalize the simultaneous component analysis (SCA) model, a canonical tool for the integrative analysis of multiple quantitative data sets, from the probabilistic perspective to explore the underlying dependence structure present in both these distinct measurements. Similar as in the SCA model, a common low dimensional subspace is assumed to represent the shared information between these two distinct measurements. However, the generalized SCA model can easily be overfit by using exact low rank constraint, leading to very large estimated parameters. We propose to use concave penalties in the low rank matrix approximation framework to mitigate this problem of overfitting and to achieve a low rank constraint simultaneously. An efficient majorization algorithm is developed to fit this model with different concave penalties. Realistic simulations (low signal to noise ratio and highly imbalanced binary data) are used to evaluate the performance of the proposed model in exactly recovering the underlying structure. Also, a missing value based cross validation procedure is implemented for model selection. In addition, exploratory data analysis of the quantitative gene expression and binary copy number aberrations (CNA) measurement obtained from the same 160 cell lines of the GDSC1000 data sets successfully show the utility of the proposed method.

**Keywords:** Data integration, SCA, binary data, low rank matrix approximation, concave penalty, majorization.

## 1 Introduction

In biological research it becomes increasingly common to have measurements of different aspects of information on the same objects to study the complex biological system [22, 13]. The resulting coupled data sets should be analyzed simultaneously to explore the dependency between variables in different data sets and to reach a global understanding of the underlying biological system. The Simultaneous Component Analysis (SCA) model is one of the canonical methods for the integrative analysis of such coupled data sets in different areas, from psychology to chemistry and biology [26]. SCA discovers the common low dimensional column subspace of the coupled quantitative data sets, and this subspace represents the shared information between them.

Besides quantitative measurement, and counts, also binary measurements are common in biological research. A binary variable has two exclusive outcomes, such as presence vs absence or true vs false, which are usually labeled as "1" and "0". However, "1" and "0" indicate abstract representations of two categories rather than quantitative values 1 and 0. Typical examples of binary measurements in biology include the measurements of point mutations, which reflect the mutation status of the DNA sequence; the binary measurements of copy number aberrations (CNA), in which "1" indicates aberrations (gains or losses of segments in chromosomal regions) occurred and "0" indicates the normal status, and the binarized DNA methylation measurements, in which "1" indicates a high level of methylation and "0" means a low level [13]. Biological binary data sets are commonly imbalanced, meaning that for most binary variables, the measurements of "0"

significantly outnumber the measurements of "1".

There is a need for statistical methods appropriate for doing the integrative analysis of coupled binary and quantitative data sets in biology research. The standard SCA models that use column centering processing steps and least squares loss criteria are not appropriate for binary data sets [26, 25]. Recently, [19] derived a factor analysis framework to model discrete and quantitative data sets simultaneously by exploiting the properties of exponential family distributions. In their framework, the special properties of binary, categorical and count data sets are taken into account in a similar way as in generalized linear models. The common low dimensional latent variables and data set specific coefficients are used to fit the discrete and quantitative data sets. For the binary data set, the Bernoulli distribution is assumed and the canonical logit link function is used. The sum of the log likelihood is used as the objective function. Furthermore, the approach allows the use of a lasso type penalty for feature selection. The Monte Carlo Newton–Raphson algorithm for this general framework, however, involves a very slow Markov Chain Monte Carlo simulation process. Both the highly complex model and the slow speed algorithm limit the possibility of explicit exploration of its properties using simulations.

In this paper, we generalize the SCA model to binary and quantitative data from a probabilistic perspective in which the high dimensional data is considered a noisy observation of a deterministic low dimensional structure, similar as in [6, 19]. We use a penalty based approach to induce the low rank structure and to control the scale of estimated parameters simultaneously. Motivated by the recent work in low rank matrix approximation under the presence of Gaussian noise [12, 14], we explore the possibility of using concave penalty functions to shrink the singular values to reach our goal. We derive a Majorization-Minimization (MM) [8, 17] based algorithm to fit the non-convex loss function. Simple closed form updates for all the parameters are derived in each iteration. Missing value based cross validation procedure is also implemented to do model selection. Our algorithm is easy to implement and guaranteed to decrease the loss function monotonically in each iteration. A detailed comparison of our method to other similar work, [19] and [28], can be found in the supplementary.

In the next sections we will generalize the SCA model for binary and quantitative data, introduce the new concave penalty and describe the majorization algorithm to estimate the model parameters. Section 4 introduces the GDSC data [13] and describes the realistic simulations we performed which are based on low signal to noise ratio and highly imbalanced binary data to evaluate the performance of the proposed SCA generalization in exactly recovering the underlying structure only from indirect binary observations and noisy quantitative observations. Section 5 introduces the cross validation approach and discusses the model evaluation measures, and in section 6, the results of the simulations and analysis of the GDSC1000 data are discussed.

## 2 The model

### Notation

$x$ : a scalar;  $\mathbf{x}(J \times 1)$ : a  $J$  dimensional column vector;  $\mathbf{X}(I \times J)$ : a matrix with  $I$  objects and  $J$  variables;  $x_{ij}$ : the  $ij$ th element of  $\mathbf{X}$ . A subscript number is added to above notations to specify the order of data sets, such as  $\mathbf{X}_1, \mathbf{X}_2$ .

### 2.1 The standard SCA model

The standard SCA model for two column centered quantitative sets of data measured on the same samples:  $\mathbf{X}_1(I \times J_1)$  and  $\mathbf{X}_2(I \times J_2)$  is expressed as

$$\begin{aligned}\mathbf{X}_1 &= \mathbf{A}\mathbf{B}_1^T + \mathbf{E}_1 \\ \mathbf{X}_2 &= \mathbf{A}\mathbf{B}_2^T + \mathbf{E}_2\end{aligned}\tag{1}$$

where  $\mathbf{A}(I \times R)$  denotes the common component scores (or latent variables), which span the common column subspace of  $\mathbf{X}_1$  and  $\mathbf{X}_2$ ;  $\mathbf{B}_1(J_1 \times R)$  and  $\mathbf{B}_2(J_2 \times R)$  are the data set specific loading

matrices for  $\mathbf{X}_1$  and  $\mathbf{X}_2$  respectively;  $\mathbf{E}_1(I \times J_1)$  and  $\mathbf{E}_2(I \times J_2)$  are residuals;  $R, R \ll \{I, J_1, J_2\}$ , is an unknown low rank. Orthogonality is imposed on  $\mathbf{A}$  to have  $\mathbf{A}^T \mathbf{A} = \mathbf{I}_R$  to have unique solutions.  $\mathbf{A}$ ,  $\mathbf{B}_1$  and  $\mathbf{B}_2$  are estimated by minimizing the sum of the squared residuals  $\mathbf{E}_1$  and  $\mathbf{E}_2$ .

## 2.2 Generalized SCA model of binary and quantitative data sets

We extend the standard SCA model to binary and quantitative data sets from a probabilistic perspective in a similar way as [24, 6]. Following the probabilistic interpretation of the PCA model [24], the high dimensional quantitative data set  $\mathbf{X}_2$  can be assumed to be a noisy observation from a deterministic low dimensional structure  $\Theta_2(I \times J_2)$  with i.i.d measurement noise,  $\mathbf{X}_2 = \Theta_2 + \mathbf{E}_2$ . Elements in  $\mathbf{E}_2(I \times J_2)$  follow a normal distribution with mean 0 and variance  $\sigma^2$ ,  $\epsilon_{2ij} \sim N(0, \sigma^2)$ . In the same way, following the interpretation of the exponential family PCA on binary data [6], we assume there is a deterministic low dimensional structure  $\Theta_1(I \times J_1)$  underlying the high dimensional binary observation  $\mathbf{X}_1$ . Elements in  $\mathbf{X}_1$  follow the Bernoulli distribution with parameters  $\phi(\Theta_1)$ ,  $x_{1ij} \sim \text{Ber}(\phi(\theta_{1ij}))$ . Here  $\phi()$  is the element wise inverse link function in the generalized linear model for binary data;  $x_{1ij}$  and  $\theta_{1ij}$  are the  $ij$ th element of  $\mathbf{X}_1$  and  $\Theta_1$  respectively. If the logit link is used,  $\phi(\theta) = (1 + \exp(-\theta))^{-1}$ , while if the probit link is used,  $\phi(\theta) = \Phi(\theta)$ , where  $\Phi$  is the cumulative density function of the standard normal distribution. Although in our paper, we only use the logit link in deriving the algorithm and in setting up the simulations, the option for the probit link is included in our implementation. The two link functions are similar, but their interpretations can be quite different [1].

In the same way as in the standard SCA model,  $\Theta_1$  and  $\Theta_2$  are assumed to lie in the same low dimensional subspace, which represents the shared information between the coupled matrices  $\mathbf{X}_1$  and  $\mathbf{X}_2$ . The commonly used column centering is not appropriate for the binary data set as the centered binary data will not be "1" and "0" anymore. Therefore, we include column offset terms  $\mu_1(J_1 \times 1)$  and  $\mu_2(J_2 \times 1)$  for a model based centering. The above ideas are modeled as

$$\begin{aligned}\Theta_1 &= \mathbf{1}\mu_1^T + \mathbf{A}\mathbf{B}_1^T \\ \Theta_2 &= \mathbf{1}\mu_2^T + \mathbf{A}\mathbf{B}_2^T\end{aligned}\tag{2}$$

where,  $\mathbf{1}(I \times 1)$  is a  $I$  dimensional vector of ones; the parameters  $\mathbf{A}$ ,  $\mathbf{B}_1$  and  $\mathbf{B}_2$  have the same meaning as in the standard SCA model and the same orthogonality constraint is imposed as  $\mathbf{A}^T \mathbf{A} = \mathbf{I}_R$ .

For the generalization to quantitative and binary coupled data, we follow the maximum likelihood estimation framework. The negative log likelihood for fitting coupled binary  $\mathbf{X}_1$  and quantitative  $\mathbf{X}_2$  is used as the objective function. In order to implement cross validation procedures based on missing value estimation [5], we introduce two weighting matrices  $\mathbf{Q}_1(I \times J_1)$  and  $\mathbf{Q}_2(I \times J_2)$  to handle the missing elements.  $q_{1ij}$  equals 0 if the  $ij$ th element in  $\mathbf{X}_1$  is missing, while it equals 1 *vice versa*. The same rules apply to  $\mathbf{Q}_2$  and  $\mathbf{X}_2$ . The loss functions  $f_1(\Theta_1)$  for fitting  $\mathbf{X}_1$  and  $f_2(\Theta_2, \sigma^2)$  for fitting  $\mathbf{X}_2$  are defined as follows:

$$\begin{aligned}f_1(\Theta_1) &= - \sum_i \sum_j q_{1ij} [x_{1ij} \log(\phi(\theta_{1ij})) + (1 - x_{1ij}) \log(1 - \phi(\theta_{1ij}))] \\ f_2(\Theta_2, \sigma^2) &= \frac{1}{2\sigma^2} \|\mathbf{Q}_2 \odot (\mathbf{X}_2 - \Theta_2)\|_F^2 + \frac{1}{2} \|\mathbf{Q}_2\|_0 \log(2\pi\sigma^2)\end{aligned}\tag{3}$$

where  $\odot$  indicates element-wise multiplication;  $\|\cdot\|_F$  is the Frobenius norm of a matrix;  $\|\cdot\|_0$  is the pseudo  $L_0$  norm of a matrix, which equals the number of nonzero elements.

The shared information between  $\mathbf{X}_1$  and  $\mathbf{X}_2$  is assumed to be fully represented by the low dimensional subspace spanned by the common component score matrix  $\mathbf{A}$ . Thus,  $\mathbf{X}_1$  and  $\mathbf{X}_2$  are conditionally independent given that the low dimensional structures  $\Theta_1$  and  $\Theta_2$  lie in the same low dimensional subspace. Therefore, the joint loss function is the direct sum of the negative log

likelihood functions for fitting  $\mathbf{X}_1$  and  $\mathbf{X}_2$ .

$$\begin{aligned}
f(\boldsymbol{\Theta}_1, \boldsymbol{\Theta}_2, \sigma^2) &= -\log(p(\mathbf{X}_1, \mathbf{X}_2 | \boldsymbol{\Theta}_1, \boldsymbol{\Theta}_2, \sigma^2)) \\
&= -\log(p(\mathbf{X}_1 | \boldsymbol{\Theta}_1) p(\mathbf{X}_2 | \boldsymbol{\Theta}_2, \sigma^2)) \\
&= -\log(p(\mathbf{X}_1 | \boldsymbol{\Theta}_1)) - \log(p(\mathbf{X}_2 | \boldsymbol{\Theta}_2, \sigma^2)) \\
&= f_1(\boldsymbol{\Theta}_1) + f_2(\boldsymbol{\Theta}_2, \sigma^2)
\end{aligned} \tag{4}$$

### 2.3 Concave surrogates of the low rank constraint

In order to arrive at meaningful solutions for the GSCA model it is necessary to introduce penalties on the estimated parameters. If we take  $\boldsymbol{\Theta} = [\boldsymbol{\Theta}_1 \ \boldsymbol{\Theta}_2]$ ,  $\boldsymbol{\mu} = [\boldsymbol{\mu}_1^T \ \boldsymbol{\mu}_2^T]^T$ , and  $\mathbf{B} = [\mathbf{B}_1 \ \mathbf{B}_2]$ , equation 2 in the generalized SCA (GSCA) model can be expressed as  $\boldsymbol{\Theta} = \mathbf{1}\boldsymbol{\mu}^T + \mathbf{A}\mathbf{B}^T$ . In the above interpretation of the GSCA model, the low rank constraint on the column centered  $\boldsymbol{\Theta}$  is expressed as the multiplication of two rank  $R$  matrices  $\mathbf{A}$ ,  $\mathbf{B}$ ,  $\mathbf{Z} = \boldsymbol{\Theta} - \mathbf{1}\boldsymbol{\mu}^T = \mathbf{A}\mathbf{B}^T$ . However, using exact low rank constraint in the GSCA model has some issues. First, the maximum likelihood estimation of this model easily leads to overfitting. Given the constraint that  $\mathbf{A}^T \mathbf{A} = \mathbf{I}$ , overfitting represents itself in a way that some elements in  $\mathbf{B}_1$  tend to divergence to positive and negative infinity. In addition, the exact low rank  $R$  in the GSCA model is commonly unknown and its selection is not straightforward.

In this paper, we take a penalty based approach to control the scale of estimated parameters and to induce low rank simultaneously. The low rank constraint on  $\mathbf{Z}$  is surrogated by a penalty function  $g(\mathbf{Z})$ , which shrinks the singular values of  $\mathbf{Z}$  to achieve a low rank structure. The most widely used convex surrogate of a low rank constraint is the nuclear norm penalty, which is simply the sum of singular values,  $g(\mathbf{Z}) = \sum_{r=1} \xi_r$  [16], where  $\xi_r$  represents the  $r$ th singular value of  $\mathbf{Z}$ . The nuclear norm penalty was also used in related work [28]. Although the convex nuclear norm penalty is easy to optimize, the same amount of shrinkage is applied to all the singular values, leading to biased estimates of the large singular values. Recent work [12, 18] already showed the superiority of concave surrogates of a low rank constraint under Gaussian noise compared to the nuclear norm penalty. Furthermore, it has shown recently that concave penalties are easier to optimize than the general non-convex problem [18]. We take  $g(\mathbf{Z}) = \sum_r g(\xi_r(\mathbf{Z}))$  as our concave surrogate of a low rank constraint on  $\mathbf{Z}$ , where  $g(\xi_r)$  is a concave penalty function of  $\xi_r$ . After replacing the low rank constraint in equation 4 by  $g(\mathbf{Z})$ , our model becomes,

$$\begin{aligned}
&\min_{\boldsymbol{\mu}, \mathbf{Z}, \sigma^2} \quad f_1(\boldsymbol{\Theta}_1) + f_2(\boldsymbol{\Theta}_2, \sigma^2) + \lambda g(\mathbf{Z}) \\
&\text{s.t. } \boldsymbol{\Theta} = \mathbf{1}\boldsymbol{\mu}^T + \mathbf{Z} \\
&\quad \boldsymbol{\Theta} = [\boldsymbol{\Theta}_1 \ \boldsymbol{\Theta}_2]
\end{aligned} \tag{5}$$

The most commonly used non-convex surrogates of a low rank constraint are concave functions, including  $L_{q:0 < q < 1}$  [11], smoothly clipped absolute deviation (SCAD) [10], a frequentist version of the generalized double Pareto (GDP) shrinkage [3] and others [18]. We include these three concave penalties in our algorithm. Their formulas and supergradients (the counterpart concept of subgradient in convex analysis, which will be used in the derivation of the algorithm) are shown in Table 1, while their thresholding properties are shown in Fig. 1.

## 3 Algorithm

Parameters  $\boldsymbol{\mu}$ ,  $\mathbf{Z}$ , and  $\sigma^2$  of the joint loss function in equation 5 are updated alternatively while fixing other parameters until reaching predefined stopping criteria. If the updating sequence follows the same order, the joint loss function is guaranteed to decrease monotonically. However, even when fixing parameters  $\boldsymbol{\mu}$  and  $\sigma^2$ , the minimization of equation 5 with respect to  $\mathbf{Z}$  is still a non-smooth and non-convex problem. We solve this problem using the MM principal [8, 17].

Table 1: Some commonly used concave penalty functions.  $\eta$  is taken as the singular value and  $q$ ,  $\lambda$  and  $\gamma$  are tuning parameters.

Penalty	Formula	Supergradient
$L_q$	$\lambda\eta^q$	$\begin{cases} +\infty & \eta = 0 \\ \lambda q\eta^{q-1} & \eta > 0 \end{cases}$
SCAD	$\begin{cases} \lambda\eta & \eta \leq \lambda \\ \frac{-\eta^2 + 2\gamma\lambda\eta - \lambda^2}{2(\gamma-1)} & \lambda < \eta \leq \gamma\lambda \\ \frac{\lambda^2(\gamma+1)}{2} & \eta > \gamma\lambda \end{cases}$	$\begin{cases} \lambda & \eta \leq \lambda \\ \frac{\gamma\lambda - \eta}{\gamma-1} & \lambda < \eta \leq \gamma\lambda \\ 0 & \eta > \gamma\lambda \end{cases}$
GDP	$\lambda \log(1 + \frac{\eta}{\gamma})$	$\frac{\lambda}{\gamma + \eta}$

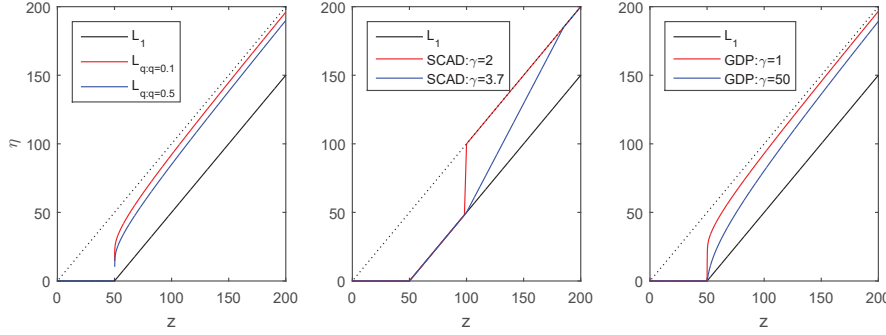


**Fig. 1** Thresholding properties of the  $L_q$ , SCAD and GDP penalties on nonnegative singular values.  $L_1$ : nuclear norm penalty.  $z$  indicates the original singular values while  $\eta$  is the value after thresholding. Although the  $L_q$  penalty works well in practice, it does not shrink the parameter continuously in the same way as, nuclear norm, SCAD and GDP penalties do.

### 3.1 The majorization of $f_1(\Theta_1) + f_2(\Theta_2, \sigma^2) + \lambda g(\mathbf{Z})$

When fixing  $\sigma^2$ , we majorize  $f(\Theta) = f_1(\Theta_1) + f_2(\Theta_2)$  to a quadratic function of  $\Theta$  by exploiting the upper bound of the second order gradient  $\nabla^2 f(\Theta)$ . In addition, concave penalty function  $g(\mathbf{Z})$  can be majorized to a linear function of the singular values by exploiting the concavity. The resulting majorized problem can be analytically solved by weighted singular value thresholding [18].

#### The majorization of $f(\Theta)$

The gradient of  $f(\Theta)$  with respect to  $\Theta$  is  $\nabla f(\Theta) = [\nabla f_1(\Theta_1) \ \nabla f_2(\Theta_2)]$ , and  $\nabla f_1(\Theta_1) = \phi(\Theta_1) - \mathbf{X}_1$  when using the logit link;  $\nabla f_2(\Theta_2) = \frac{1}{\sigma^2}(\Theta_2 - \mathbf{X}_2)$ . We first assume the universal upper bound of the second order gradient  $\nabla^2 f(\Theta)$  is  $L$ , and a proper value will be found by a line search method. We have the following inequality

$$\begin{aligned}
f(\Theta) &\leq f(\Theta^k) + \text{tr}(\nabla f(\Theta^k)^T(\Theta - \Theta^k)) + \frac{L}{2}\|\Theta - \Theta^k\|_F^2 \\
&= \frac{L}{2}\|\Theta - \mathbf{H}^k\|_F^2 + c \\
\mathbf{H}^k &= \Theta^k - \frac{1}{L}\nabla f(\Theta^k)
\end{aligned} \tag{6}$$

in which  $\Theta^k$  is the approximation of  $\Theta$  during  $k$ th iteration and  $c$  is a constant. When taking into account the missing values, the majorized function in equation 6 becomes  $\frac{L}{2}\|\mathbf{Q} \odot (\Theta - \mathbf{H}^k)\|_F^2$ , in which  $\mathbf{Q} = [\mathbf{Q}_1 \ \mathbf{Q}_2]$ . Following [15], we further majorize the weighted least squares function

$\frac{L}{2} \|\mathbf{Q} \odot (\boldsymbol{\Theta} - \mathbf{H}^k)\|_F^2$  into a quadratic function of  $\boldsymbol{\Theta}$  as

$$\begin{aligned} & \frac{L}{2} \|\mathbf{Q} \odot (\boldsymbol{\Theta} - \mathbf{H}^k)\|_F^2 \\ & \leq \frac{L}{2} \|\boldsymbol{\Theta} - \widetilde{\mathbf{H}}^k\|_F^2 + c \\ & \widetilde{\mathbf{H}}^k = \mathbf{Q} \odot \mathbf{H}^k + \mathbf{Q}^c \odot \boldsymbol{\Theta}^k \end{aligned} \tag{7}$$

where  $\mathbf{Q}^c$  is the element-wise binary complement of  $\mathbf{Q}$ .

### A proper value of $L$

We implemented a backtracking line search method in a similar way as in [4] to select a proper value of  $L_k$  in each iteration. The initialization is  $L_0 = \frac{\|\nabla f(\boldsymbol{\Theta}^0)\|_F}{\|\boldsymbol{\Theta}^0\|_F}$ , in which  $\boldsymbol{\Theta}^0$  is the initial value of  $\boldsymbol{\Theta}$  and  $\nabla f(\boldsymbol{\Theta}^0)$  is its gradient. The value of  $L_k$  doubles when the condition  $\boldsymbol{\Theta}_{\text{pre}} = \boldsymbol{\Theta}^k - \frac{1}{L_k} \nabla f(\boldsymbol{\Theta}^k)$ ,  $f(\boldsymbol{\Theta}_{\text{pre}}) \leq f(\boldsymbol{\Theta}^k) + \text{tr}(\nabla f(\boldsymbol{\Theta}^k)^T (\boldsymbol{\Theta}_{\text{pre}} - \boldsymbol{\Theta}^k)) + \frac{L_k}{2} \|\boldsymbol{\Theta}_{\text{pre}} - \boldsymbol{\Theta}^k\|_F^2$  is not satisfied. Otherwise, the value of  $L_k$  will be updated as  $L_{k+1} = 0.9L_k$ .

### The majorization of $g(\mathbf{Z})$

Let  $g(\xi_r)$  be a concave function. From the definition of concavity, we have  $g(\xi_r) \leq g(\xi_r^k) + \omega_r^k (\xi_r - \xi_r^k) = \omega_r^k \xi_r + c$ , in which  $\xi_r^k = \xi_r(\mathbf{Z}^k)$  is the  $r$ th singular value of the  $k$ th approximation  $\mathbf{Z}^k$ ,  $\omega_r^k \in \partial g(\xi_r^k)$  and  $\partial g(\xi_r^k)$  is the set of supergradients of function  $g()$  at  $\xi_r^k$ . For all the concave penalties in our paper, their supergradient is unique, thus  $\omega_r^k = \partial g(\xi_r^k)$ . Therefore,  $g(\mathbf{Z}) = \sum_r g(\xi_r(\mathbf{Z}))$  can be majorized as follows

$$\begin{aligned} g(\mathbf{Z}) &= \sum_r g(\xi_r(\mathbf{Z})) \\ &\leq \sum_r \omega_r^k \xi_r + c \\ \omega_r^k &= \partial g(\xi_r(\mathbf{Z}^k)) \end{aligned} \tag{8}$$

### The majorization of $f(\boldsymbol{\Theta}) + \lambda g(\mathbf{Z})$

To summarize the above results,  $f(\boldsymbol{\Theta}) + \lambda g(\mathbf{Z})$  has been majorized to the following function.

$$\begin{aligned} & \frac{L}{2} \|\boldsymbol{\Theta} - \widetilde{\mathbf{H}}^k\|_F^2 + \lambda \sum_r \omega_r^k \xi_r + c \\ & \boldsymbol{\Theta} = \mathbf{1}\boldsymbol{\mu}^T + \mathbf{Z} \\ & \mathbf{H}^k = \boldsymbol{\Theta}^k - \frac{1}{L} \nabla f(\boldsymbol{\Theta}^k) \\ & \widetilde{\mathbf{H}}^k = \mathbf{Q} \odot \mathbf{H}^k + \mathbf{Q}^c \odot \boldsymbol{\Theta}^k \\ & \omega_r^k = \partial g(\xi_r(\mathbf{Z}^k)) \end{aligned} \tag{9}$$

## 3.2 Generalized alternating minimization

We optimize  $\boldsymbol{\mu}$ ,  $\mathbf{Z}$  and  $\sigma^2$  alternately while fixing the other parameters. However, the updating of  $\boldsymbol{\mu}$  and  $\mathbf{Z}$  depends on solving the majorized problem in equation 9 rather than solving the original problem in equation 5. Because of the MM principle, this step will also monotonically decrease the original loss function in equation 5.

### Updating $\boldsymbol{\mu}$

The analytical solution of  $\boldsymbol{\mu}$  in equation 9 is simply the column mean of  $\widetilde{\mathbf{H}}^k$ ;  $\boldsymbol{\mu} = \frac{1}{I} \widetilde{\mathbf{H}}^k{}^T \mathbf{1}$ .

### Updating $\mathbf{Z}$

After removing the offset term  $\boldsymbol{\mu}$ , the loss function in equation 9 becomes  $\frac{L}{2}\|\mathbf{Z} - \mathbf{J}\widetilde{\mathbf{H}}^k\|_F^2 + \lambda \sum_r \omega_r^k \xi_r$ , in which  $\mathbf{J} = \mathbf{I} - \frac{1}{I}\mathbf{1}\mathbf{1}^T$  is the column centering matrix. The solution of the resulting problem is equivalent to the proximal operator of the weighted sum of singular values, which has an analytical form solution [18]. Suppose  $\mathbf{USV}^T = \mathbf{J}\widetilde{\mathbf{H}}^k$  is the SVD decomposition of  $\mathbf{J}\widetilde{\mathbf{H}}^k$ , the analytical form solution of  $\mathbf{Z}$  is  $\mathbf{Z} = \mathbf{US}_{\omega\lambda/L}\mathbf{V}^T$ , in which  $\mathbf{S}_{\omega\lambda/L} = \text{Diag}\{(s_{rr} - \lambda\omega_r/L)_+\}$  and  $s_{rr}$  is the  $i$ th diagonal element in  $\mathbf{S}$ .

### Updating $\sigma^2$

By setting the gradient of  $f(\boldsymbol{\Theta}, \sigma^2)$  in equation 5 with respect to  $\sigma^2$  to be 0, we have the following analytical solution of  $\sigma^2$ ,  $\sigma^2 = \frac{1}{\|\mathbf{Q}_2\|_0} \|\mathbf{Q}_2 \odot (\mathbf{X}_2 - \boldsymbol{\Theta}_2)\|_F^2$ . When no low rank estimation of  $\mathbf{Z}$  can be achieved, the constructed model is close to a saturated model and the estimated  $\hat{\sigma}^2$  is close to 0. In that case, when  $\hat{\sigma}^2 < 0.05$ , the algorithm stops and gives a warning that a low rank estimation has not been achieved.

### Initialization and stopping criteria

Random initialization is used. All the elements in  $\mathbf{Z}^0$  are sampled from the standard uniform distribution,  $\boldsymbol{\mu}^0$  is set to 0 and  $(\sigma^2)^0$  is set to 1. The relative change of the objective value is used as the stopping criteria.

## 3.3 Pseudocode

Pseudocode of the algorithm described above is shown in algorithm 1.  $\epsilon_f$  is the tolerance of relative change of the loss function.

---

**Algorithm 1** A MM algorithm for fitting the GSCA model with concave penalties.

---

**Input:**  $\mathbf{X}_1, \mathbf{X}_2$ , penalty,  $\lambda, \gamma$ ;

**Output:**  $\hat{\boldsymbol{\mu}}, \hat{\mathbf{Z}}, \hat{\sigma}^2$ ;

- 1: Compute  $\mathbf{Q}_1, \mathbf{Q}_2$  and  $\mathbf{Q} = [\mathbf{Q}_1 \ \mathbf{Q}_2]$  for missing values in  $\mathbf{X}_1$  and  $\mathbf{X}_2$ ;
  - 2: Initialize  $\boldsymbol{\mu}^0, \mathbf{Z}^0, (\sigma^2)^0, L_0$ ;
  - 3:  $k = 0$ ;
  - 4: **while**  $(f^{k-1} - f^k)/f^{k-1} > \epsilon_f$  **do**
  - 5:    $\nabla f_1(\boldsymbol{\Theta}_1^k) = \phi(\boldsymbol{\Theta}_1^k) - \mathbf{X}_1$ ;  $\nabla f_2(\boldsymbol{\Theta}_2^k) = \frac{1}{(\sigma^2)^k}(\boldsymbol{\Theta}_2^k - \mathbf{X}_2)$ ;
  - 6:    $\nabla f(\boldsymbol{\Theta}^k) = [\nabla f_1(\boldsymbol{\Theta}_1^k), \nabla f_2(\boldsymbol{\Theta}_2^k)]$ ;
  - 7:   Finding a proper  $L_k$  using the backtracking line search;
  - 8:    $\mathbf{H}^k = \boldsymbol{\Theta}^k - \frac{1}{L_k} \nabla f(\boldsymbol{\Theta}^k)$ ;
  - 9:    $\widetilde{\mathbf{H}}^k = \mathbf{Q} \odot \mathbf{H}^k + \mathbf{Q}^c \odot \boldsymbol{\Theta}^k$ ;
  - 10:    $\omega_r^k = \partial g(\xi_r(\mathbf{Z}^k))$ ;
  - 11:    $\boldsymbol{\mu}^{k+1} = \frac{1}{I}(\widetilde{\mathbf{H}}^k)^T \mathbf{1}$ ;
  - 12:    $\mathbf{USV}^T = \mathbf{J}\widetilde{\mathbf{H}}^k$ ;
  - 13:    $\mathbf{S}_{\lambda\omega/L_k} = \text{Diag}\{(s_{rr} - \lambda\omega_r/L_k)_+\}$ ;
  - 14:    $\mathbf{Z}^{k+1} = \mathbf{US}_{\lambda\omega/L_k}\mathbf{V}^T$ ;
  - 15:    $\boldsymbol{\Theta}^{k+1} = \mathbf{1}(\boldsymbol{\mu}^{k+1})^T + \mathbf{Z}^{k+1}$ ;
  - 16:    $[\boldsymbol{\Theta}_1^{k+1} \ \boldsymbol{\Theta}_2^{k+1}] = \boldsymbol{\Theta}^{k+1}$ ;
  - 17:    $(\sigma^2)^{k+1} = \frac{1}{\|\mathbf{Q}_2\|_0} \|\mathbf{Q}_2 \odot (\mathbf{X}_2 - \boldsymbol{\Theta}_2^{k+1})\|_F^2$ ;
  - 18:    $k = k + 1$ ;
  - 19: **end while**
-

### 3.4 A special case

When  $q$  in the  $L_q$  penalty is set to 1, we have the nuclear norm penalty  $g(\mathbf{Z}) = \sum_r \xi_r(\mathbf{Z})$ . As  $g(\mathbf{Z})$  is a linear function of the singular values of  $\mathbf{Z}$ , it is both convex and concave. In addition, the majorization of  $g(\mathbf{Z})$  in equation 8 is  $g(\mathbf{Z})$  itself. Thus, when setting  $q$  in  $L_q$  to 1, our algorithm simplifies to a MM algorithm to optimize the GSCA model with nuclear norm penalty. Since this is a convex problem, the global optimum can be found.

## 4 Real data set and simulation process

### 4.1 Real data set

The Genomic Determinants of Sensitivity in Cancer 1000 (GDSC1000) [13] contains 926 cell lines with comprehensive measurements of point mutation, CNA, methylation and gene expression. We selected the binary CNA and quantitative gene expression measurements on the same cell lines (each cell line is a sample) as an example to show the GSCA model. To simplify the interpretation of the derived model, only the cell lines of three cancer types, BRCA (breast invasive carcinoma, 48 human cell lines), LUAD (lung adenocarcinoma, 62 human cell lines) and SKCM (skin cutaneous melanoma, 50 human cell lines), are included. The CNA data set has 410 binary variables. Each variable is a copy number region of the chromosome, in which "1" indicates aberration happened in this region while "0" indicates the normal status. The binary CNA data set is very imbalanced, which is a common phenomenon in biological research. Of the binary CNA data set, there is 6.66% "1" in total. The empirical marginal probabilities of binary CNA variables are shown in Fig. S1. The quantitative gene expression data set contains 17420 variables, of which 1000 gene expression variables with the largest variance are selected. After that, the gene expression data is column centered and scaled to make it more consistent with the assumption of the GSCA model.

### 4.2 Simulation process

Motivated by [7], we defined the signal to ratio (SNR) for generating binary data according to the latent variable interpretation of the generalized linear models of binary data. Elements in  $\mathbf{X}_1$  are independent and indirect binary observations of the corresponding elements in an underlying quantitative matrix  $\mathbf{X}_1^*(I \times J_1)$ ,  $x_{1ij} = 1$  if  $x_{1ij}^* > 0$  and  $x_{1ij} = 0$  *vice versa*. Quantitative  $\mathbf{X}_1^*$  can be expressed as  $\mathbf{X}_1^* = \boldsymbol{\Theta}_1 + \mathbf{E}_1$ , in which  $\boldsymbol{\Theta}_1 = \mathbf{1}\boldsymbol{\mu}_1^T + \mathbf{A}\mathbf{B}_1^T$ , and elements in  $\mathbf{E}_1$  follow the standard logistic distribution,  $\epsilon_{1ij} \sim \text{Logistic}(0, 1)$ . The SNR for generating binary data  $\mathbf{X}_1$  is defined as  $\text{SNR}_1 = \frac{\|\mathbf{A}\mathbf{B}_1^T\|_F^2}{\|\mathbf{E}_1\|_F^2}$ . Assume the quantitative  $\mathbf{X}_2$  is simulated as  $\mathbf{X}_2 = \boldsymbol{\Theta}_2 + \mathbf{E}_2$ , in which  $\boldsymbol{\Theta}_2 = \mathbf{1}\boldsymbol{\mu}_2^T + \mathbf{A}\mathbf{B}_2^T$  and elements in  $\mathbf{E}_2$  follow a normal distribution with 0 mean and  $\sigma^2$  variance,  $\epsilon_{2ij} \sim N(0, \sigma^2)$ . The SNR for generating quantitative  $\mathbf{X}_2$  is defined as  $\text{SNR}_2 = \frac{\|\mathbf{A}\mathbf{B}_2^T\|_F^2}{\|\mathbf{E}_2\|_F^2}$ .

After the definition of the signal to noise ratio (SNR), we show how to simulate the coupled binary  $\mathbf{X}_1$  and quantitative  $\mathbf{X}_2$  following the GSCA model with logit link with pre-specified SNRs.  $\boldsymbol{\mu}_1$  represents the logit transform of the marginal probabilities of binary variables and  $\boldsymbol{\mu}_2$  represents the mean of the marginal distributions of quantitative variables. They can be simulated according to the characteristic of real biological data set. The score matrix  $\mathbf{A}$  and loading matrices  $\mathbf{B}_1, \mathbf{B}_2$  can be simulated in the following manner. First, we express  $\mathbf{A}\mathbf{B}_1^T$  and  $\mathbf{A}\mathbf{B}_2^T$  in a SVD type as  $\mathbf{A}\mathbf{B}_1^T = \mathbf{U}\mathbf{D}_1\mathbf{V}_1^T$  and  $\mathbf{A}\mathbf{B}_2^T = \mathbf{U}\mathbf{D}_2\mathbf{V}_2^T$ , in which  $\mathbf{U}^T\mathbf{U} = \mathbf{I}_R$ ,  $\mathbf{D}_1$  and  $\mathbf{D}_2$  are diagonal matrices,  $\mathbf{V}_1^T\mathbf{V}_1 = \mathbf{I}_R$  and  $\mathbf{V}_2^T\mathbf{V}_2 = \mathbf{I}_R$ . All the elements in  $\mathbf{U}$ ,  $\mathbf{V}_1$  and  $\mathbf{V}_2$  are independently sampled from the standard normal distribution. After that they are orthogonalized by the QR algorithm. Then a diagonal matrix  $\mathbf{D}(R \times R)$  is simulated. Its decreasing nonnegative diagonal elements are simulated as follows.  $R$  elements are sampled from standard normal distribution, then transformed to positive by taking their absolute values and sorted in a decreasing order. After that,  $\mathbf{D}$  is scaled as  $\mathbf{D}_1 = c_1\mathbf{D}$  and  $\mathbf{D}_2 = c_2\mathbf{D}$  by positive scalars  $c_1$  and  $c_2$  to satisfy the pre-specified  $\text{SNR}_1$  and  $\text{SNR}_2$ . Then, binary elements in  $\mathbf{X}_1$  are sampled from the Bernoulli distribution with corresponding parameter  $\phi(\theta_{1ij})$ , in which  $\phi()$  is inverse logit function and  $\boldsymbol{\Theta}_1 = \mathbf{1}\boldsymbol{\mu}_1^T + \mathbf{A}\mathbf{B}_1^T$ . Quantitative data set  $\mathbf{X}_2$  is generated as  $\mathbf{X}_2 = \boldsymbol{\Theta}_2 + \mathbf{E}_2$ , in which  $\boldsymbol{\Theta}_2 = \mathbf{1}\boldsymbol{\mu}_2^T + \mathbf{A}\mathbf{B}_2^T$  and elements in  $\mathbf{E}_2$  are



sampled from  $N(0, \sigma^2)$ .

## 5 Evaluation metric and model selection

As for simulated data sets, the true parameters  $\Theta = [\Theta_1 \ \Theta_2]$ ,  $\mu = [\mu_1^T \mu_1^T]^T$  and  $Z = AB^T$  are available, the generalization error of the constructed model can be evaluated by comparing the true parameters and their model estimates. Thus, the evaluation metric is defined as the relative least squared error (RLSE) of the model parameters.

The RLSE of estimating  $\Theta$ , is defined as  $RLSE(\Theta) = \frac{\|\Theta - \hat{\Theta}\|_F^2}{\|\Theta\|_F^2}$ , where  $\Theta$  represents the true parameter and  $\hat{\Theta}$  its GSCA model estimate. The RLSE of  $\mu$  and  $Z$ , are expressed as  $RLSE(\mu)$  and  $RLSE(Z)$  and they are defined in the same way as for  $\Theta$ .

For real data sets, K-fold missing value based cross validation (CV) is used to estimate the generalization error of the constructed model. In order to make the prediction of the left out fold elements independent to the constructed model based on the reminding folds, the data is partitioned into K folds of elements which are selected in a diagonal style rather than row wise from  $X_1$  and  $X_2$  respectively, similar to the leave out patterns described by Wold [27, 5]. The test set elements of each fold in  $X_1$  and  $X_2$  are taken as missing values, and the remaining data are used to construct a GSCA model. After estimation of  $\hat{\Theta}$  and  $\hat{\sigma}^2$  are obtained from the constructed GSCA model, the negative log likelihood of using  $\hat{\Theta}$ ,  $\hat{\sigma}^2$  to predict the missing elements (left out fold) is recorded. This negative log likelihood is scaled by the number of missing elements. This process is repeated K times until all the K folds have been left out once. The mean of the K scaled negative log likelihoods is taken as the CV error.

When we define  $X = [X_1 \ X_2]$  and  $J = J_1 + J_2$ , the penalty term  $\lambda g(Z)$  is not invariant to the number of non-missing elements in  $X$ , as the joint loss function (equation 4) is the sum of the log likelihoods for fitting all the non-missing elements in the data  $X$ . Therefore, by setting one fold of elements to be missing during CV process,  $\frac{\|X\|_0}{J \times J} \lambda$  rather than  $\lambda$  is used as the amount of penalty. During the K-fold CV process, a warm start strategy, using the results of previous constructed model as the initialization of next model, is applied. In this way, the K-fold CV can be greatly accelerated. The speed of the GSCA models with different penalties using different stopping criteria, and the corresponding CV procedure, are fully characterized in Table S1.

In the model selection process, the tuning parameter  $\lambda$  and hyper-parameters ( $q$  in  $L_q$  and  $\gamma$  in SCAD and GDP) can be selected by a grid search. However, previous work of using these penalty functions in supervised learning context [11, 10, 3] and our experiments have shown that the results are not very sensitive to the selection of these hyper-parameters, and thus a default value can be set. On the other hand, the selection of tuning parameter  $\lambda$  does have a significant effect on the results, and should be optimized by the grid search.

## 6 Experiments

### 6.1 Overfitting of the GSCA model with exact low rank constraint

In our first simulation experiment we use coupled binary CNA and quantitative gene expression data sets. The developed algorithm in this paper can be easily modified to fit a GSCA model with an exact low rank constraint and orthogonality constraint  $AA^T = I$  (details are discussed in the supplementary material). GSCA models with three components with exact rank constraint are fitted using stopping criteria  $\epsilon_f = 1e-5$  and  $\epsilon_f = 1e-8$ . In both cases the exact same initialization is used. As shown in Fig. 2, different stopping criteria can greatly effect the estimated  $\hat{B}_1$  from the GSCA models. Furthermore, the number of iterations to reach convergence has increased from 146 to 20343. Similar phenomena have been observed in logistic linear regression and logistic PCA [9, 23]. In logistic linear regression, the estimated coefficients corresponding to the directions where two classes are linearly separable tend to go to positive infinity or negative infinity. The overfitting

issue of the GSCA model with exact low rank constraint can be interpreted in the same way by taking the columns of score matrix  $\mathbf{A}$  as the latent variables and the loading matrix  $\mathbf{B}_1$  as the coefficients to fit the binary  $\mathbf{X}_1$ . Thus, if an exact low rank constraint is preferred, an extra size penalty should be added on  $\mathbf{B}_1$  to avoid overfitting.

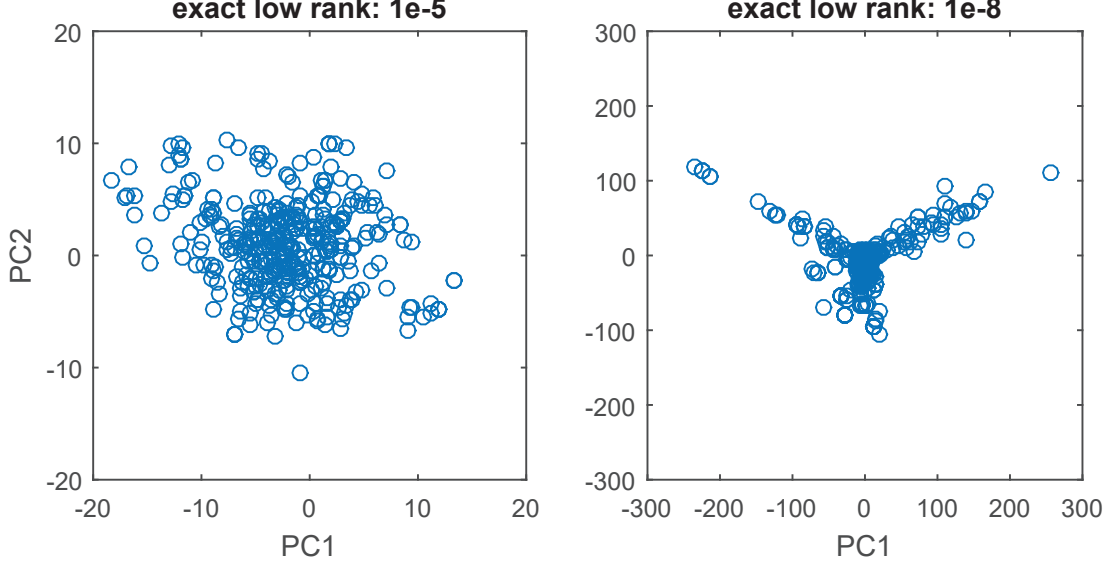


**Fig. 2** Loading plots of estimated  $\hat{\mathbf{B}}_1$  from the GSCA models with exact low rank constraint using two different stopping criteria  $\epsilon_f = 10^{-5}$  and  $\epsilon_f = 10^{-8}$ .

## 6.2 Concave penalty for the GSCA model leads to lower generalization error than the nuclear norm penalty

Motivated from the challenging situation (very imbalanced binary data and low signal to noise ratio) in biology research, we set up the simulation as follows. Simulated  $\mathbf{X}_1$  and  $\mathbf{X}_2$  have the same size as the real data sets,  $I = 160$ ,  $J_1 = 410$ ,  $J_2 = 1000$ . The logit transform of the empirical marginal probabilities of the CNA data is set as  $\mu_1$ . Elements in  $\mu_2$  are sampled from the standard normal distribution. The rank  $R$  of the common subspace is set to  $R = 10$ ;  $\sigma^2$  is set to 1;  $\text{SNR}_1$  and  $\text{SNR}_2$  are set to 1. After the simulation of  $\mathbf{X}_1$ , two columns with identical “0” patterns were removed.

As the GSCA model with the nuclear norm penalty is a convex problem, the global optimum can be obtained. The nuclear norm penalty is therefore used as the baseline in the comparison with other penalties. An interval from  $\lambda_0$  large enough to achieve an estimated rank of at most rank 1, to  $\lambda_t$ , small enough to achieve an estimated rank of 160, is selected based on low precision models ( $\epsilon_f = 10^{-2}$ ). 50 values of  $\lambda$  are selected equally from the interval  $[\lambda_0, \lambda_t]$ . The convergence criterion is set as  $\epsilon_f = 10^{-8}$ . The results are shown in Fig. 3. With the decrease of  $\lambda$ , the estimated rank of  $(\hat{\mathbf{Z}})$  increased from 0 to 160, and the estimated  $\hat{\sigma}^2$  decreased from 2 to close to 0. The minimum  $\text{RLSE}(\Theta)$  of 0.185 (the corresponding  $\text{RLSE}(\mu)$  and  $\text{RLSE}(\mathbf{Z})$  are 0.074 and 0.451 respectively) can be achieved at  $\log_{10}(\lambda) = 1.59$ , which corresponds to  $\text{rank}(\hat{\mathbf{Z}}) = 44$  and  $\hat{\sigma}^2 = 0.954$ . There are sharp transitions in all the three subplots near the point  $\log_{10}(\lambda) = 1.586$ . The reason is that when penalty is not large enough, the estimated rank becomes 159, the constructed GSCA model is almost a saturated model. Thus the model has high generalization error and the estimated  $\hat{\sigma}^2$  also becomes close to 0. Given that we only have indirect binary observation  $\mathbf{X}_1$  and highly noisy observation  $\mathbf{X}_2$ , the performance of GSCA model with nuclear norm penalty is reasonable. However, results can be greatly improved by using concave penalties.

For concave penalties, different values of the hyper-parameters,  $q$  in  $L_q$ ,  $\gamma$  in SCAD and GDP, are selected according to their thresholding properties. For each value of the hyper-parameter,

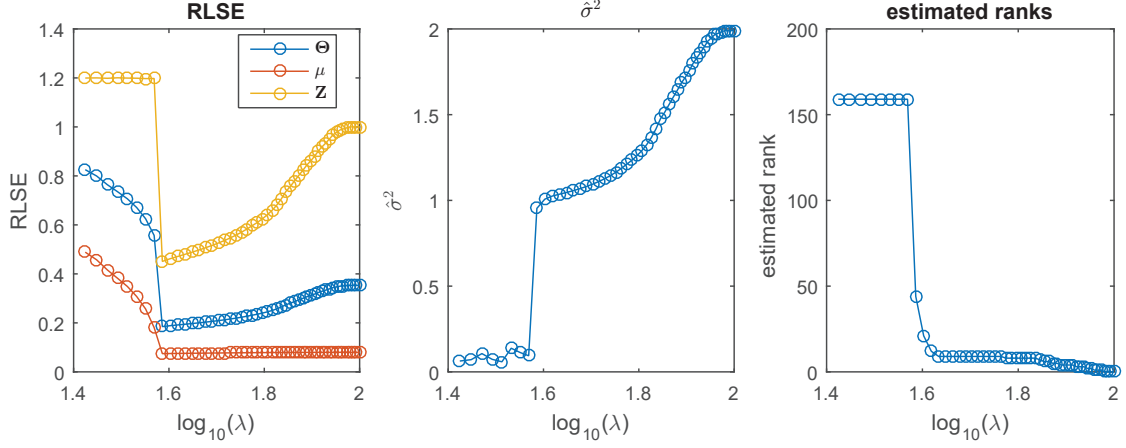


**Fig. 3** RLSEs in estimating  $\Theta$ ,  $\mu$ ,  $\mathbf{Z}$  (left), the estimated  $\hat{\sigma}^2$  (center) and the estimated rank( $\hat{\mathbf{Z}}$ ) (right) from the GSCA model with nuclear norm penalty as a function of the tuning parameter  $\lambda$ .

values of tuning parameter  $\lambda$  are selected in the same manner as described above. The minimum  $\text{RLSE}(\Theta)$  achieved and the corresponding  $\text{RLSE}(\mu)$  and  $\text{RLSE}(\mathbf{Z})$  for different values of hyper-parameter of the GSCA models with different penalty functions are shown in Fig. 4. The relationship between RLSEs,  $\lambda$  and hyper-parameter for the GSCA model with  $L_q$ , SCAD and GDP penalty functions are fully characterized in Fig. S2, Fig. S3 and Fig. S4 respectively. As shown in Fig. 4, all GSCA models with concave penalties can achieve much lower RLSEs in estimating  $\Theta$ ,  $\mu$  and  $\mathbf{Z}$  compared to the convex nuclear norm penalty. Among the three concave penalties used,  $L_q$  and GDP have better performance.

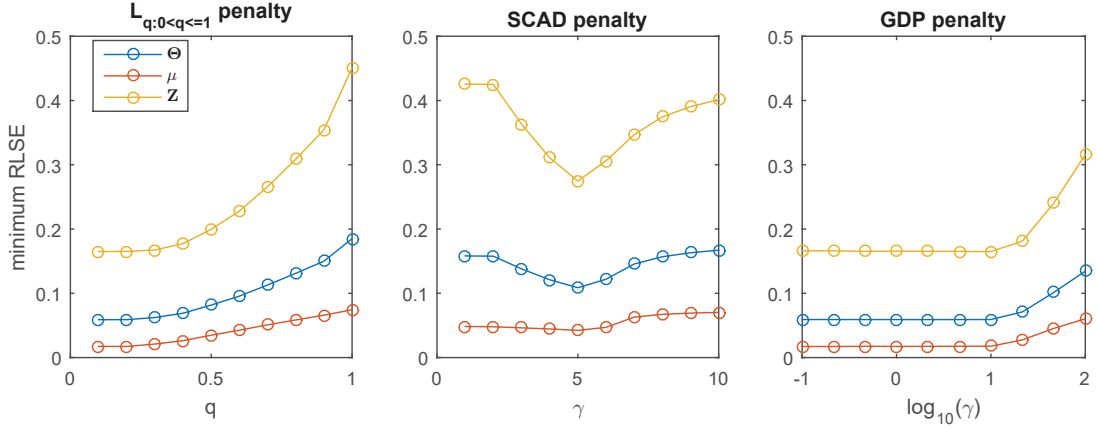


**Fig. 4** The minimum  $\text{RLSE}(\Theta)$  achieved and the corresponding  $\text{RLSE}(\mu)$  and  $\text{RLSE}(\mathbf{Z})$  for different values of hyper-parameter for  $L_q$  penalty (left), for SCAD penalty (center) and for GDP penalty (right). The legends indicate the RLSEs in estimating  $\Theta$ ,  $\mu$  and  $\mathbf{Z}$  respectively.

If we get access to the full information, the underlying quantitative data  $\mathbf{X}_1^*$  rather than the binary observation  $\mathbf{X}_1$ , the SCA model on  $\mathbf{X}_1^*$  and  $\mathbf{X}_2$  is simply a PCA model on  $[\mathbf{X}_1^* \ \mathbf{X}_2]$ . From this model, we can get an estimation of  $\Theta$ ,  $\mu$  and  $\mathbf{Z}$ . We compared the results derived from the SCA model on the full information, the GSCA models with nuclear norm,  $L_{q:q=0.2}$ , SCAD ( $\gamma = 5$ ) and GDP ( $\gamma = 1$ ) penalties. All the models are selected to achieve the minimum  $\text{RLSE}(\Theta)$ . The RLSEs of estimating  $\Theta$ ,  $\mu$  and  $\mathbf{Z}$  and the rank of estimated  $\hat{\mathbf{Z}}$  from different models are shown in Table 2. Here we can see that the GSCA models with  $L_{q:q=0.2}$  and GDP ( $\gamma = 1$ ) penalties have better performance in almost all criteria compared to the nuclear norm and SCAD penalties, and even comparable with the SCA model on full information. The singular values of the true  $\mathbf{Z}$ , estimated  $\hat{\mathbf{Z}}$  from the above models and the noise terms  $\mathbf{E} = [\mathbf{E}_1 \ \mathbf{E}_2]$  are shown in Fig. 5. Only the

first 15 singular values are shown to have higher resolution of the details. Since the 10<sup>th</sup> singular value of the simulated data  $\mathbf{Z}$  is smaller than the noise level, the best achievable rank estimation is 9. Both the  $L_{q;q=0.2}$  and GDP ( $\gamma = 1$ ) penalties successfully find the correct rank 9, and they have a very good approximation of the first 9 singular values of  $\mathbf{Z}$ . On the other hand, the nuclear norm penalty shrinks all the singular values too much. Furthermore, the SCAD penalty overestimates the first three singular values and therefore shrinks all the other singular values too much. These results are easily understandable if taking their thresholding properties in Fig. 2 into account. Both the  $L_q$  and the GDP penalties have very good performance in this simulation experiment.

Table 2: The RLSEs of estimating  $\Theta$ ,  $\mu$  and  $\mathbf{Z}$  and the rank of estimated  $\hat{\mathbf{Z}}$  from different models.

	RLSE( $\Theta$ )	RLSE( $\mu$ )	RLSE( $\mathbf{Z}$ )	rank( $\hat{\mathbf{Z}}$ )
$L_1$	0.185	0.074	0.451	44
$L_{q;q=0.2}$	0.059	0.017	0.165	9
SCAD( $\gamma = 5$ )	0.109	0.042	0.275	35
GDP( $\gamma = 1$ )	0.059	0.017	0.166	9
full information	0.022	0.005	0.072	9

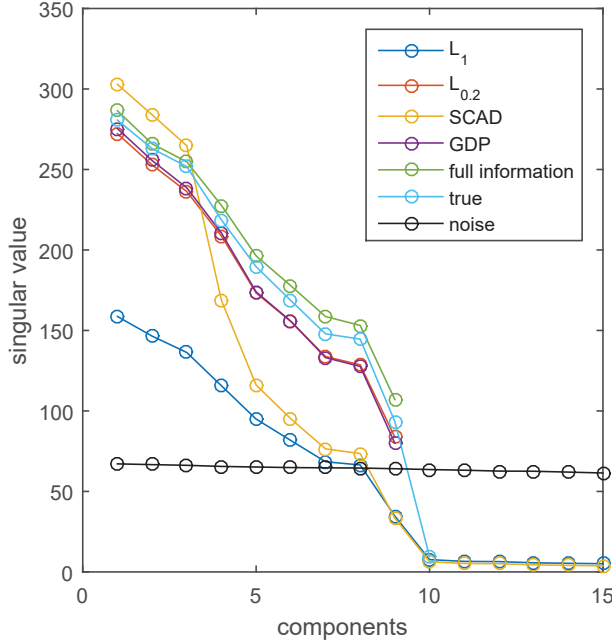


**Fig. 5** Approximation of the singular values using different penalties in the simulation experiment. “ $L_1$ ”, “ $L_{0.2}$ ”, “SCAD”, “GDP”, “full information” indicate the singular values of estimated  $\hat{\mathbf{Z}}$  from the corresponding models; “true” indicates the singular values of the simulated  $\mathbf{Z}$ ; “noise” indicates the singular values of the noise term  $\mathbf{E}$ , which has full rank.

### 6.3 The GSCA model with GDP penalty is more robust to imbalanced binary data compared to the iCluster+ model

We compared our GSCA model with GDP penalty to iCluster+ model from [19] on simulated data sets. The parameters for the GSCA model with GDP penalty is the same as described above. The running time is 80.6s when  $\epsilon_f = 1^{-8}$ , and 12.3s when  $\epsilon_f = 1^{-5}$ . For the iCluster+ model, 9 latent variables are specified. The tuning parameter of the lasso type constraint on the data specific coefficient matrices are set to 0. The default convergence criteria (the maximum of the absolute changes of the estimated parameters in two sequent iterations is less than  $1e-4$ ) is used. The running time is close to 3 hours. The constructed iCluster+ model provides the estimation of

column offset  $\hat{\mu}$ , the common latent variables  $\hat{\mathbf{A}}$ , and data set specific coefficient matrices  $\hat{\mathbf{B}}_1$  and  $\hat{\mathbf{B}}_2$ . The estimated  $\hat{\mathbf{Z}}$  and  $\hat{\Theta}$  are computed in the same way as defined in the model section. The RLSEs in estimating  $\Theta$ ,  $\mu$  and  $\mathbf{Z}$  for iCluster+ are 2.52, 2.47 and 3.07 respectively. Compared to the results from the GSCA models in Table 2, iCluster+ is unable to provide good results on the simulated data sets. Fig. S5 compared the estimated  $\hat{\mu}_1$  from the GSCA model with GDP penalty and iCluster+ model. As shown in Fig. S5 (right), the iCluster+ model is unable to estimate the offset  $\mu$  correctly. Many elements of estimated  $\hat{\mu}_1$  are exactly 0, which corresponds to an estimated marginal probability of 0.5. In addition, as shown in Fig. 6 (left), the singular values of the estimated  $\hat{\mathbf{Z}}$  from the iCluster+ model are clearly overestimated. These undesired results from the iCluster+ model are due mainly to the unbalancedness of the simulated binary data set. If the offset term  $\mu_1$  in the simulation is set to 0, which corresponds to balanced binary data simulation, and fix all the other parameters in the same way as in the above simulation, the results of iCluster+ and GSCA with GDP penalty are more comparable. In that case the RLSEs of estimating  $\Theta$ ,  $\mu$  and  $\mathbf{Z}$  in the GSCA model with GDP penalty are 0.071, 0.036 and 0.096 respectively, while the RLSEs of the iCluster+ model are 0.107, 0.046 and 0.146 respectively. As shown in Fig. 6(right), the singular values of estimated  $\hat{\mathbf{Z}}$  from the iCluster+ model are much more accurate compared to the imbalanced case. However, iCluster+ still overestimates the singular values compared to the GSCA model with GDP penalty. This phenomenon is related to the fact that exact low rank constraint is also used in the iCluster+ model.

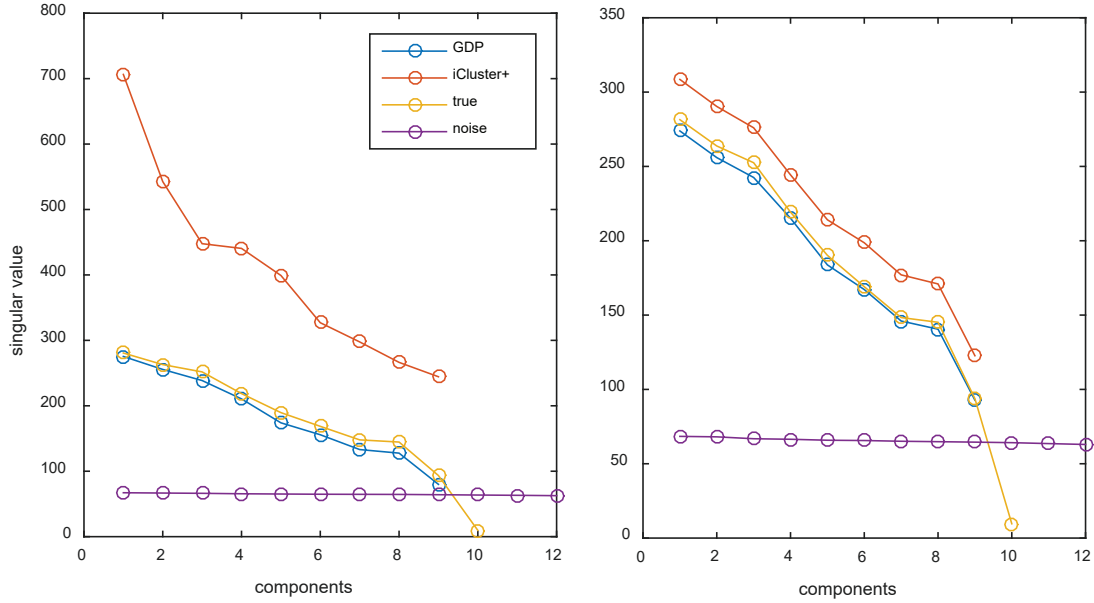


**Fig. 6** The singular values of estimated  $\hat{\mathbf{Z}}$  using the iCluster+ model and the GSCA model with GDP penalty on the simulation with imbalanced binary data (left) and with balanced binary data (right).

#### 6.4 The performance of the GSCA model for the simulation with different signal to noise ratios

In this section we will explore the performance of the GSCA model for data with varying noise levels. Equal SNR levels are used in the simulation for  $\mathbf{X}_1$  and  $\mathbf{X}_2$ . 20 SNR values are selected from the interval  $[0.1, 100]$  with equal steps in log space. Then we simulated coupled binary data  $\mathbf{X}_1$  and quantitative  $\mathbf{X}_2$  using the different SNRs in the same way as described above. During this process, except for the parameters  $c_1$  and  $c_2$ , which are used to adjust the SNRs, all other parameters used in the simulation were kept the same. The GSCA model with GDP penalty ( $\gamma = 1$ ), with the nuclear norm penalty, and the SCA model on the full information (defined above) are used in these simulation experiments. For these three models, the model selection process was done in the same way as described above. The models with the minimum RLSE( $\Theta$ ) are selected.

As shown in Fig. 7, the GSCA model with GDP penalty always has better performance than the convex nuclear norm penalty, and it is comparable to the situation where the full information is available. With the increase of SNR, the  $\text{RLSE}(\mathbf{Z})$  derived from the GSCA model, which is used to evaluate the performance of the model in recovering the underlying low dimensional structure, first decreases to a minimum and then increases. Although this result counterparts the intuition that larger SNR means higher quality of data, it is in line with previous results on logistic PCA model on binary data set [7]. In order to understand this effect, considering the S-shaped logistic curve, the plot of the function  $\phi(\theta) = (1 + \exp(-\theta))^{-1}$ . This curve almost becomes flat when  $\theta$  becomes very large. There is no resolution anymore in these flat regimes. A large deviation in  $\theta$  has almost no effect on the logistic response. When the SNR becomes extremely large, the scale of the simulated parameter  $\theta$  is very extreme, then even if we have a good estimation of the probability  $\hat{\pi} = \phi(\hat{\theta})$ , the scale of estimated  $\hat{\theta}$  can be far away from the simulated  $\theta$ . We refer [7] for a detailed interpretation of this phenomenon.

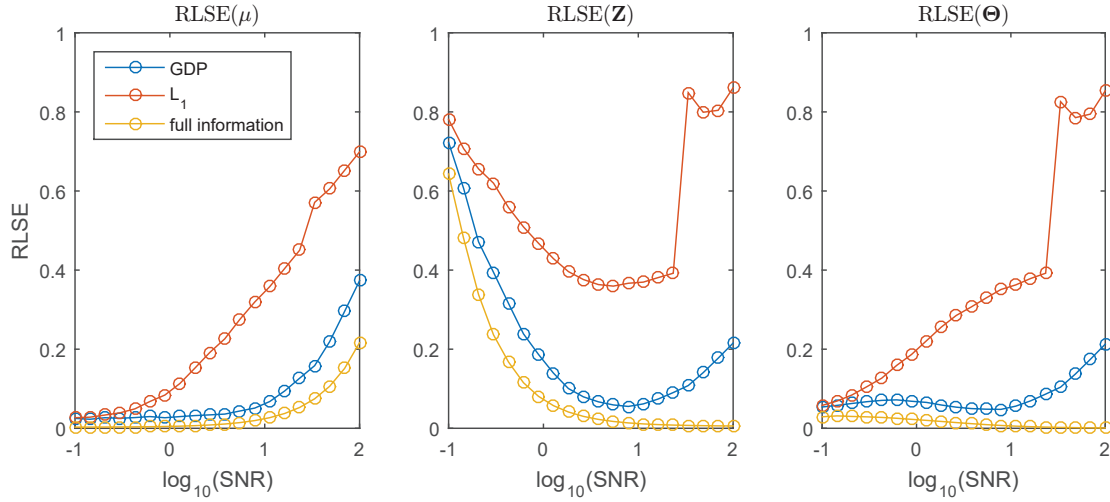


**Fig. 7** Minimum  $\text{RLSE}(\Theta)$  (right), and the corresponding  $\text{RLSE}(\mu)$  (left),  $\text{RLSE}(\mathbf{Z})$  (center), of the GSCA model with nuclear norm penalty (legend  $L_1$ ), GDP penalty (legend GDP), and SCA model on full information (legend full information) for different SNR levels.

## 6.5 Assessing the model selection procedure

The cross validation procedure and the cross validation error have been defined in the model selection section. The GSCA model with GDP penalty is used as an example to assess the model selection procedure.  $\epsilon_f = 10^{-5}$  is used as the stopping criteria for all the following experiments to save time. The values of  $\lambda$  and  $\gamma$  are selected in the same way as was described in section 6.2. Fig. 8 shows the minimum  $\text{RLSE}(\Theta)$  and minimum CV error achieved for different values of the hyper-parameter  $\gamma$ . The minimum CV error changes in a similar way as the minimum  $\text{RLSE}(\Theta)$  with respect to the values of  $\gamma$ . However, taking into account the uncertainty of estimated CV errors, the difference of the minimum CV errors for different  $\gamma$  is very small. Thus, we recommend to fix  $\gamma$  to be 1, rather than using cross validation to select it. Furthermore, setting  $\gamma = 1$  as the default value for the GDP penalty has a probabilistic interpretation as was discussed in [3].

In situation where the GSCA model is used for exploratory data analysis, there is no need to select  $\lambda$  explicitly. It is sufficient to find a proper value to achieve a two or three components GSCA model, in order to visualize the estimated score and loading matrices. If the goal is confirmatory data analysis, it is possible to select the tuning parameter  $\lambda$  explicitly by the proposed cross validation procedure. Fig. 9 shows how the tuning parameter  $\lambda$  effects the CV errors,  $\text{RLSE}(\Theta)$  and the estimated ranks. The minimum CV error obtained is close to the Bayes error, which is the scaled negative log likelihood in cases where the true parameters  $\Theta$  and  $\sigma^2$  are known. As shown in Fig. 9(right), the mean of the estimated ranks (CV) from the different K-folds during the cross

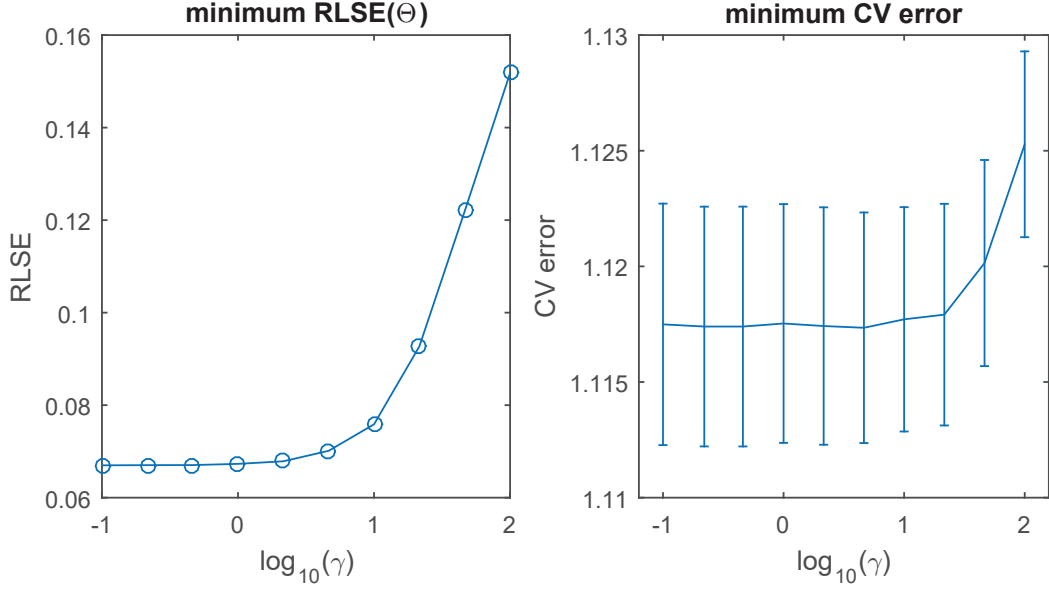


**Fig. 8** Minimum RLSE( $\Theta$ ) (left) and minimum CV error (right) for different values of  $\gamma$  from the GSCA model with GDP penalty. One standard error bars are added to the CV error plot.

validation procedure, and the estimated ranks (fit) from the full data sets can be different even after we have already adapted the value of  $\lambda$  according to the number of non-missing elements in cross validation process. Also the estimated rank plot (Fig. 9 right) explains the observed inconsistency between CV error plot (Fig. 9 left) and the RLSE( $\Theta$ ) plot (Fig. 9 center). However, usually the estimated rank (fit), corresponding to the minimum RLSE( $\Theta$ ), and the estimated rank (CV), corresponding to the minimum CV error, are the same. Therefore, we suggest to use the proposed CV procedure to select a rank estimate according to the value of  $\lambda$  at which the minimum CV error is obtained. Finally, we can select a similar value of  $\lambda$  to achieve the same rank estimation for the full data.

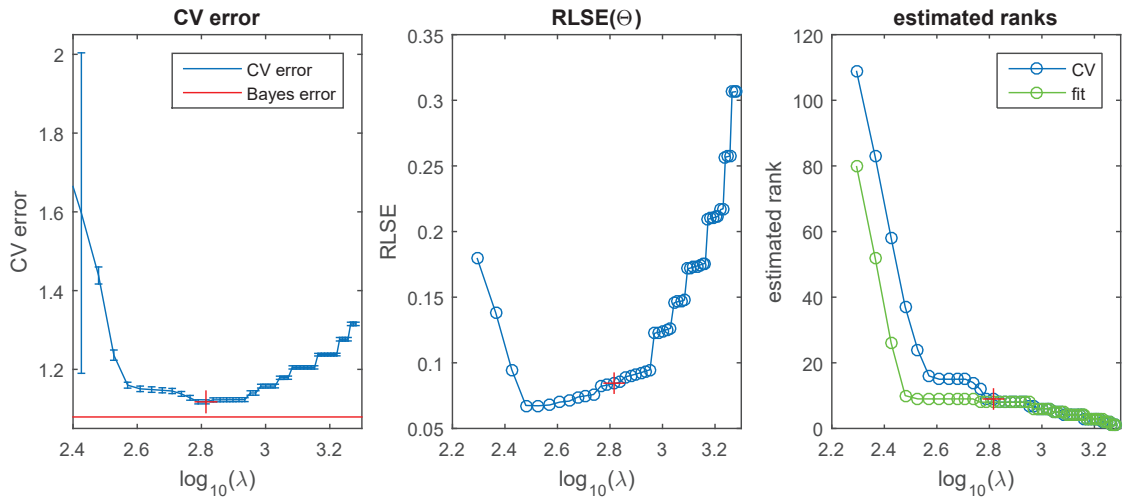


**Fig. 9** Crossvalidation error, RLSE and estimated rank for different values of the tuning parameter  $\lambda$ . “Bayes error” indicates the mean log negative likelihood using simulated  $\Theta$  and  $\sigma^2$  to fit the simulated data sets  $\mathbf{X}_1$  and  $\mathbf{X}_2$ . The red cross marker indicates the point where the minimum CV error is achieved. “fit” and “CV” (right plot) indicate the mean rank( $\hat{\mathbf{Z}}$ ) derived from the models constructed in K-fold cross validation and the rank( $\hat{\mathbf{Z}}$ ) derived from a model constructed on full data set without missing elements.



## 6.6 Exploratory data analysis of the coupled CNA and gene expression data sets

Finally, We applied the GSCA model (with GDP penalty and  $\gamma=1$ ) to the GDSC data set of 160 tumor cell lines that have been profiled for both binary CNA ( $160 \times 410$ ) and quantitative gene expression ( $160 \times 1000$ ). The results of model selection (Fig. S6) validate the existence of a low dimensional common structure between CNA and gene expression data sets. However, for exploratory purposes, we will construct a three components model instead.

We first considered the score plot resulting from this GSCA model. The first two PCs show a clear clustering by cancer type (Fig. 10 left), and in some cases even subclusters (i.e. hormone-positive breast cancer, MITF-high melanoma). These results suggest that the GSCA model captures the relevant biology in these data. Interestingly, when we performed PCA on the gene expression data, we obtained score plots that were virtually identical to those resulting from GSCA (Fig.S7 left, modified RV coefficient: 0.9998), suggesting that this biological relevance is almost entirely derived from the gene expression data.

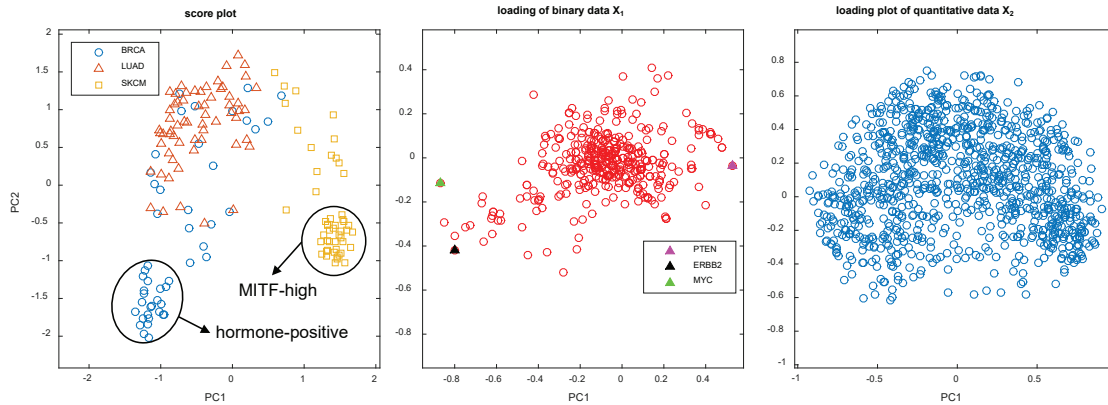


**Fig. 10** Score plot (left), loading plot for binary CNA data  $X_1$  (center) and loading plot for gene expression data  $X_2$  (right) derived from the constructed GSCA model. The legends BRCA, LUAD and SKCM indicate the cancer types of different samples. The samples inside the MITF-high circle indicate MITF-high melanoma cell lines; those inside the hormone-high circle indicate hormone-positive breast cancer cell lines. The legends PTEN, ERBB2 and MYC are the CNA features, which are useful for the interpretation of GSCA model.

We then wondered whether the GSCA model could leverage the gene expression data to help us gain insight into the CNA data. To test this, we first established how much insight could be gained from the CNA data in isolation. Fig.S8 shows the scores and loadings from a three components logistic PCA model [9] applied to the CNA data. While these do seem to contain structure in the loading plot, we believe that they mostly explain technical characteristics of the data. For example, deletions and amplifications are almost perfectly separated from each other by the  $PC1=0$  line in the loading plot (Fig. S9). Additionally, the scores on PC1 are strongly associated to the number of copy number aberrations (i.e. to the number of 1s) in a given sample (Fig. S10). Finally, the clusters towards the left of the loading plot suggested two groups of correlated features, but these could trivially be explained by genomic position, i.e. these features correspond to regions on the same chromosome arm, which are often completely deleted or amplified) (Fig. S11). Following these observations, we believe that a study of the CNA data in isolation provides little biological insight.

On the other hand, using the GSCA model's CNA loadings (Fig. 10 center), we could more easily relate the features to the biology. Let us focus on features with extreme values on PC1 and for which the corresponding chromosomal region contains a known driver gene. For example, the position of MYC amplifications in the loading plot indicates that MYC amplifications occur mostly in lung adenocarcinoma and breast cancer samples (Fig. 10 center; Fig. S12). Similarly, ERBB2 amplifications were indicated to occur mainly in breast cancer samples (Fig. 10 center; Fig. S12).



Finally, PTEN deletions were enriched in melanomas, though the limited size of the loading also indicates that they are not exclusive to melanomas (Fig. 10 center; Fig. S12). Importantly, these three findings are in line with known biology [2, 21, 20] and hence exemplify how GSCA could be used to interpret the CNA data. Altogether, using the GSCA model, we were able to 1) capture the biological relevance in the gene expression data, and 2) leverage that biological relevance from the gene expression to gain a better understanding of the CNA data.

## 7 Discussion

In this paper, we generalized the standard SCA model to explore the dependence between coupled binary and quantitative data sets. However, the GSCA model with exact low rank constraint overfits the data, as some estimated parameters tend to diverge to positive infinity or negative infinity. Therefore, concave penalties, nuclear norm (both convex and concave),  $L_q$ , SCAD and GDP are introduced in the low rank approximation framework to achieve low rank approximation and to mitigate the overfitting issues of the GSCA model. An efficient algorithm framework with analytical form updates for all the parameters is developed to optimize the GSCA model with any concave penalties. All concave penalties used in our experiments have better performance with respect to generalization error and estimated low rank of the constructed GSCA model compared to the nuclear norm penalty. Both  $L_q$  and GDP penalties with proper model selection can recover the simulated low rank structures almost exactly only from indirect binary observation  $\mathbf{X}_1$  and noisy quantitative observation  $\mathbf{X}_2$ . Furthermore we have shown that the GSCA model outperforms the iCluster+ model with respect to speed and accuracy of the estimation of the model parameters.

Now why does the GDP approach work so well. The exact low rank constraint thresholds the singular values in a hard manner, in which as a result only the largest  $R$  singular values are kept. On the other hand, nuclear norm penalty works in a soft manner, in which all the singular values are shrunk by the same amount of  $\lambda$ . The thresholding properties of the concave penalties discussed in this paper lie in between these two approaches. As  $\mathbf{Z} = \mathbf{A}\mathbf{B}$  and  $\mathbf{A}^T\mathbf{A} = \mathbf{I}_R$ , the scale of the loadings is related to the scale of the singular values of  $\mathbf{Z}$  as  $\|\mathbf{B}\|_F^2 = \|\mathbf{B}_1\|_F^2 + \|\mathbf{B}_2\|_F^2 = \sum_r^R \xi_r(\mathbf{Z})^2$ . Thus, we can shrink the singular values of  $\mathbf{Z}$  to control the scale of estimated loading matrices in an indirect way. The exact low rank constraint kept the  $R$  largest singular values but without control of the scale of the estimated singular values, leading to overfitting. On the other hand, nuclear norm penalty shrinks all the singular values to the same amount of  $\lambda$ , leading to biased estimation of the singular values. A proper penalty, like  $L_q$  or GDP, achieves a balance in thresholding the singular values. Among the concave penalties we used in the experiment, the SCAD penalty does not work well in the given examples. The reason is that the SCAD penalty does not shrink the large singular values, which therefore tend to be overfitted, while the smaller singular values are shrunk too much.

Compared to the iCluster+ method, only the option of binary and quantitative data sets are included in our GSCA model, and at the moment no sparsity can be imposed for the integrative analysis of binary and quantitative data sets. However, the GSCA model with GDP penalty is optimized by a more efficient algorithm, it is much more robust to the imbalanced nature of the biological binary data and it provides a much better performance for the simulation experiments in this paper. Furthermore, the exploratory analysis of the GDSC coupled CNA and gene expression data sets provided important information on the binary CNA data that was not obtained by a separate analysis.

## References

- [1] Alan Agresti. *Categorical data analysis*. John Wiley & Sons, 2013.
- [2] Rehan Akbani, Kadir C Akdemir, B Arman Aksoy, Monique Albert, Adrian Ally, Samir Kumar B Amin, Harindra Arachchi, Arshi Arora, J Todd Auman, Brenda Ayala, et al. Genomic classification of cutaneous melanoma. *Cell*, 161(7):1681–1696, 2015.

- [3] Artin Armagan, David B Dunson, and Jaeyong Lee. Generalized double pareto shrinkage. *Statistica Sinica*, 23(1):119, 2013.
- [4] Stephen R Becker, Emmanuel J Candès, and Michael C Grant. Templates for convex cone problems with applications to sparse signal recovery. *Mathematical programming computation*, 3(3):165, 2011.
- [5] Rasmus Bro, Karin Kjeldahl, AK Smilde, and HAL Kiers. Cross-validation of component models: a critical look at current methods. *Analytical and bioanalytical chemistry*, 390(5):1241–1251, 2008.
- [6] Michael Collins, Sanjoy Dasgupta, and Robert E Schapire. A generalization of principal components analysis to the exponential family. In *Advances in neural information processing systems*, pages 617–624, 2002.
- [7] Mark A Davenport, Yaniv Plan, Ewout Van Den Berg, and Mary Wootters. 1-bit matrix completion. *Information and Inference: A Journal of the IMA*, 3(3):189–223, 2014.
- [8] Jan De Leeuw. Block-relaxation algorithms in statistics. In *Information systems and data analysis*, pages 308–324. Springer, 1994.
- [9] Jan de Leeuw. Principal component analysis of binary data: applications to roll-call-analysis. 2011.
- [10] Jianqing Fan and Runze Li. Variable selection via nonconcave penalized likelihood and its oracle properties. *Journal of the American statistical Association*, 96(456):1348–1360, 2001.
- [11] Wenjiang J Fu. Penalized regressions: the bridge versus the lasso. *Journal of computational and graphical statistics*, 7(3):397–416, 1998.
- [12] Matan Gavish and David L Donoho. Optimal shrinkage of singular values. *IEEE Transactions on Information Theory*, 63(4):2137–2152, 2017.
- [13] Francesco Iorio, Theo A Knijnenburg, Daniel J Vis, Graham R Bignell, Michael P Menden, Michael Schubert, Nanne Aben, Emanuel Gonçalves, Syd Barthorpe, Howard Lightfoot, et al. A landscape of pharmacogenomic interactions in cancer. *Cell*, 166(3):740–754, 2016.
- [14] Julie Josse and Sylvain Sardy. Adaptive shrinkage of singular values. *Statistics and Computing*, 26(3):715–724, 2016.
- [15] Henk AL Kiers. Weighted least squares fitting using ordinary least squares algorithms. *Psychometrika*, 62(2):251–266, 1997.
- [16] Vladimir Koltchinskii, Karim Lounici, Alexandre B Tsybakov, et al. Nuclear-norm penalization and optimal rates for noisy low-rank matrix completion. *The Annals of Statistics*, 39(5):2302–2329, 2011.
- [17] Kenneth Lange. *MM optimization algorithms*, volume 147. SIAM, 2016.
- [18] Canyi Lu, Changbo Zhu, Chunyan Xu, Shuicheng Yan, and Zhouchen Lin. Generalized singular value thresholding. In *AAAI*, pages 1805–1811, 2015.
- [19] Qianxing Mo, Sijian Wang, Venkatraman E Seshan, Adam B Olshen, Nikolaus Schultz, Chris Sander, R Scott Powers, Marc Ladanyi, and Ronglai Shen. Pattern discovery and cancer gene identification in integrated cancer genomic data. *Proceedings of the National Academy of Sciences*, 110(11):4245–4250, 2013.
- [20] Cancer Genome Atlas Network et al. Comprehensive molecular portraits of human breast tumours. *Nature*, 490(7418):61, 2012.
- [21] Cancer Genome Atlas Research Network et al. Comprehensive molecular profiling of lung adenocarcinoma. *Nature*, 511(7511):543, 2014.
- [22] Cancer Genome Atlas (TCGA) Research Network et al. Comprehensive genomic characterization defines human glioblastoma genes and core pathways. *Nature*, 455(7216):1061, 2008.

- [23] Yipeng Song, Johan A Westerhuis, Nanne Aben, Magali Michaut, Lodewyk FA Wessels, and Age K Smilde. Principal component analysis of binary genomics data. *Briefings in Bioinformatics*, 2017.
- [24] Michael E Tipping and Christopher M Bishop. Probabilistic principal component analysis. *Journal of the Royal Statistical Society: Series B (Statistical Methodology)*, 61(3):611–622, 1999.
- [25] Robert A van den Berg, Iven Van Mechelen, Tom F Wilderjans, Katrijn Van Deun, Henk AL Kiers, and Age K Smilde. Integrating functional genomics data using maximum likelihood based simultaneous component analysis. *BMC bioinformatics*, 10(1):340, 2009.
- [26] Katrijn Van Deun, Age K Smilde, Mariët J van der Werf, Henk AL Kiers, and Iven Van Mechelen. A structured overview of simultaneous component based data integration. *BMC bioinformatics*, 10(1):246, 2009.
- [27] Svante Wold. Cross-validatory estimation of the number of components in factor and principal components models. *Technometrics*, 20(4):397–405, 1978.
- [28] Dingming Wu, Dongfang Wang, Michael Q Zhang, and Jin Gu. Fast dimension reduction and integrative clustering of multi-omics data using low-rank approximation: application to cancer molecular classification. *BMC genomics*, 16(1):1022, 2015.

# Supplementary for "Generalized Simultaneous Component Analysis of Binary and Quantitative data"

## GSCA model with exact low rank constraint

The exact low rank constraint on  $\mathbf{Z}$  can be expressed as the multiplication of two low rank matrices  $\mathbf{A}$  and  $\mathbf{B}$ . The optimization problem related to the GSCA model with exact low rank constraint can be expressed as

$$\begin{aligned} \min_{\boldsymbol{\mu}, \mathbf{Z}, \sigma^2} \quad & f_1(\boldsymbol{\Theta}_1) + f_2(\boldsymbol{\Theta}_2, \sigma^2) \\ \text{s.t.} \quad & \boldsymbol{\Theta} = \mathbf{1}\boldsymbol{\mu}^T + \mathbf{Z} \\ & \boldsymbol{\Theta} = [\boldsymbol{\Theta}_1 \ \boldsymbol{\Theta}_2] \\ & \text{rank}(\mathbf{Z}) = R \end{aligned} \tag{10}$$

The developed algorithm in the paper can be slightly modified to fit this model. Same as in the paper, the above optimization problem can be majorized to the following problem.

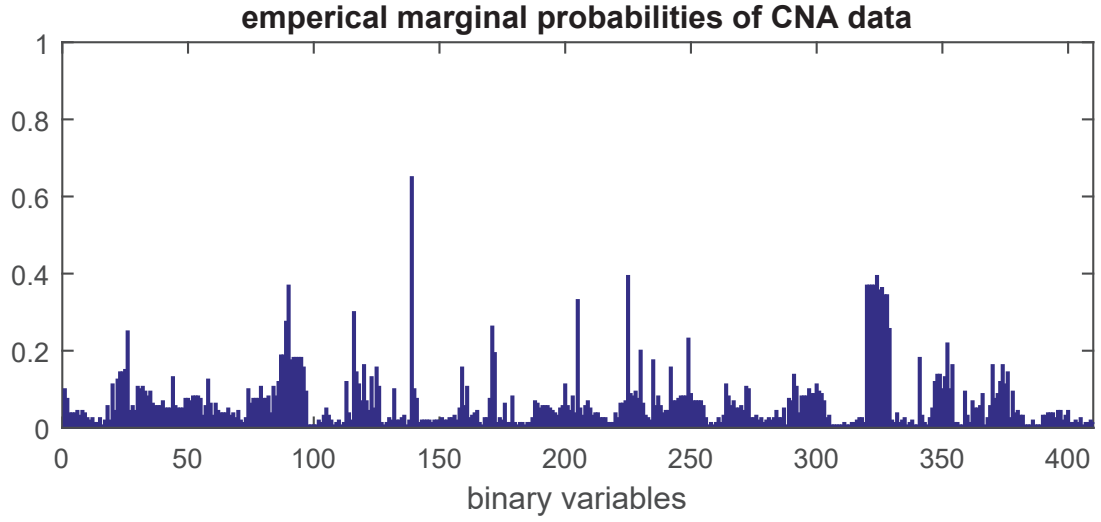
$$\begin{aligned} & \frac{L}{2} \|\boldsymbol{\Theta} - \widetilde{\mathbf{H}}^k\|_F^2 + c \\ & \boldsymbol{\Theta} = \mathbf{1}\boldsymbol{\mu}^T + \mathbf{Z} \\ & \mathbf{H}^k = \boldsymbol{\Theta}^k - \frac{1}{L} \nabla f(\boldsymbol{\Theta}^k) \\ & \widetilde{\mathbf{H}}^k = \mathbf{Q} \odot \mathbf{H}^k + \mathbf{Q}^c \odot \boldsymbol{\Theta}^k \\ & \text{rank}(\mathbf{Z}) = R \end{aligned} \tag{11}$$

The analytical solution of the  $\boldsymbol{\mu}$  is also the column mean of  $\widetilde{\mathbf{H}}^k$ . After deflating out the offset term, the majorized problem becomes  $\min_{\mathbf{Z}} \frac{L}{2} \|\mathbf{Z} - \mathbf{J}\widetilde{\mathbf{H}}^k\|_F^2$  s.t.  $\text{rank}(\mathbf{Z}) = R$ . The global optimal solution is the  $R$  truncated SVD of  $\mathbf{J}\widetilde{\mathbf{H}}^k$ . Other steps in the algorithm to fit the GSCA model with exact low rank constraint are exactly the same the algorithm developed in the paper to fit the GSCA model with concave penalty.

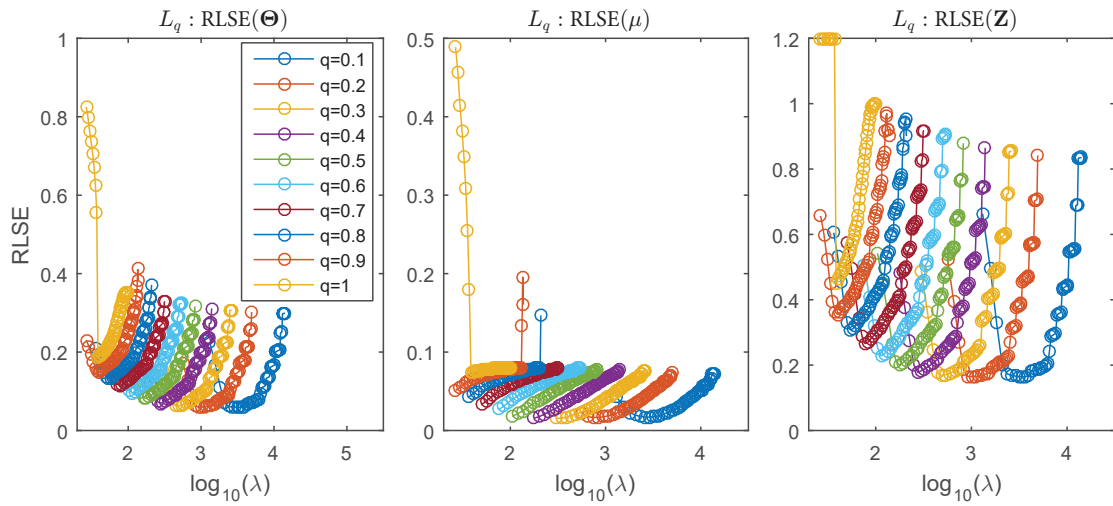
## Figures and tables

Table S1: Comparison of the average computational time (in seconds) of the GSCA model with different penalties and the corresponding 7-fold CV procedure. The binary CNA and quantitative gene expression data sets are used as an example. "fit": a three components GSCA model; "CV": 7-fold CV procedure. All the models are repeated 5 times, the average computational time is recorded. All the computations are performed on a laptop with an i5-5300U CPU, 8GB RAM, 64-bit Windows 10 system and MATLAB of R2015a.

penalty	$\epsilon_f = 1e - 5$	$\epsilon_f = 1e - 8$
$L_1$ : fit	12.24	74.04
$L_1$ : CV	20.27	
$L_{0.2}$ : fit	13.59	89.46
$L_{0.2}$ : CV	31.58	
SCAD( $\gamma = 5$ ): fit	12.17	73.7
SCAD( $\gamma = 5$ ): CV	20.74	
GDP( $\gamma = 1$ ): fit	14.54	90.54
GDP( $\gamma = 1$ ): CV	33.98	



**Fig. S1** Empirical marginal probabilities of binary CNA data set.



**Fig. S2** Relationship between  $q$ ,  $\lambda$  and RLSEs of estimating  $\Theta$ ,  $\mu$  and  $Z$  achieved for the GSCA model with  $L_q$  penalty.

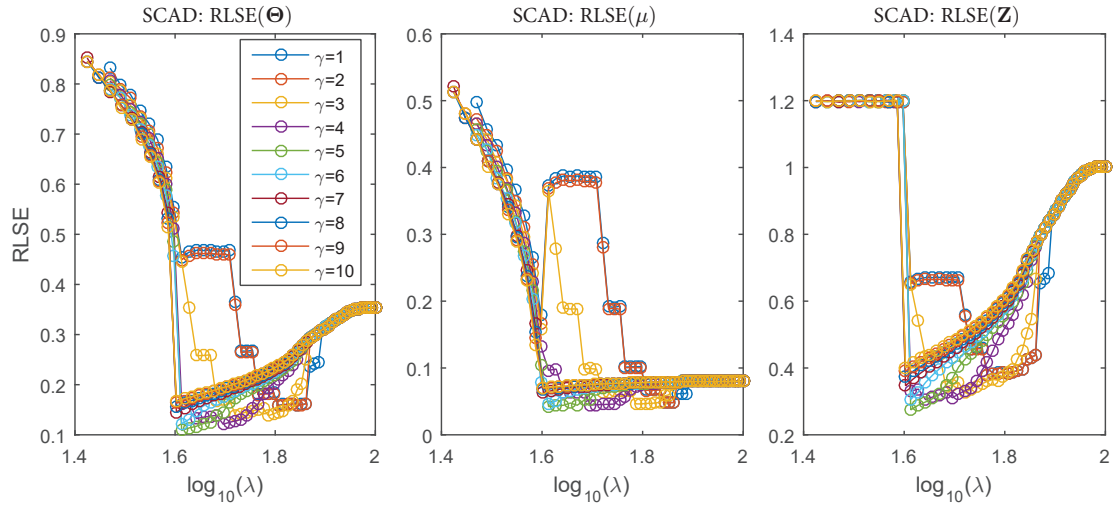


**Fig. S3** Relationship between  $\gamma$ ,  $\lambda$  and RLSEs of estimating  $\Theta$ ,  $\mu$  and  $Z$  achieved for the GSCA model with SCAD penalty.

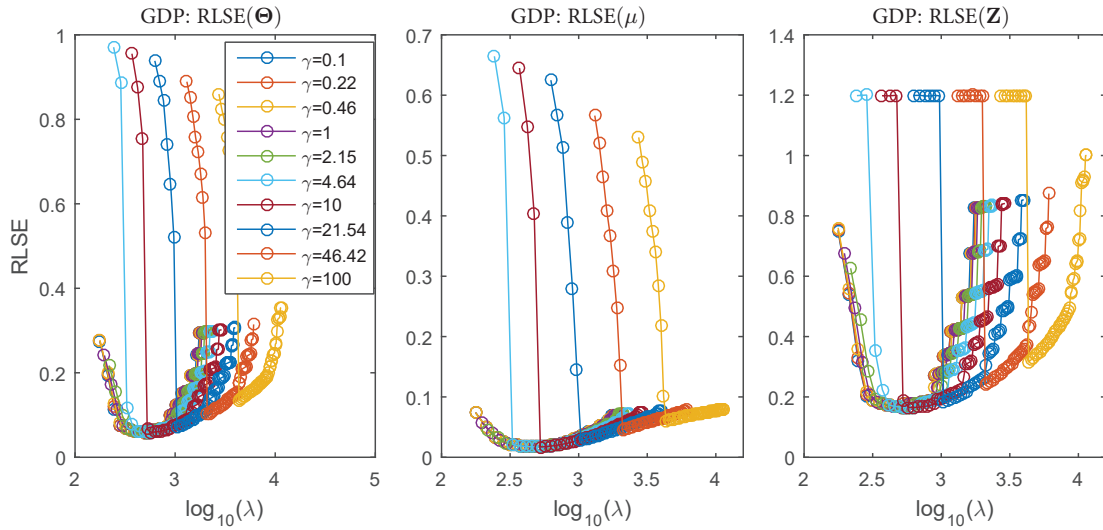


**Fig. S4** Relationship between  $\gamma$ ,  $\lambda$  and RLSEs of estimating  $\Theta$ ,  $\mu$  and  $Z$  achieved for the GSCA model with GDP penalty.

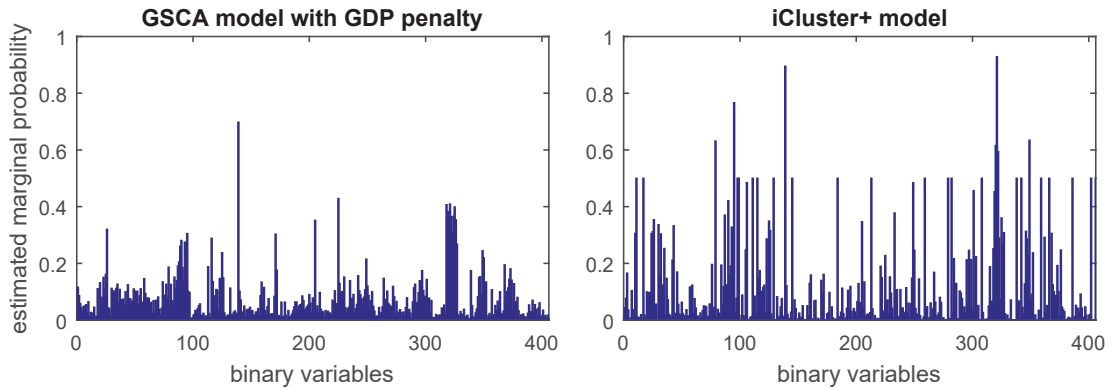


**Fig. S5** Estimated marginal probabilities (the logit transform of the estimated  $\hat{\mu}_1$ ) from the GSCA model with GDP penalty (left) and iCluster+ model (right).

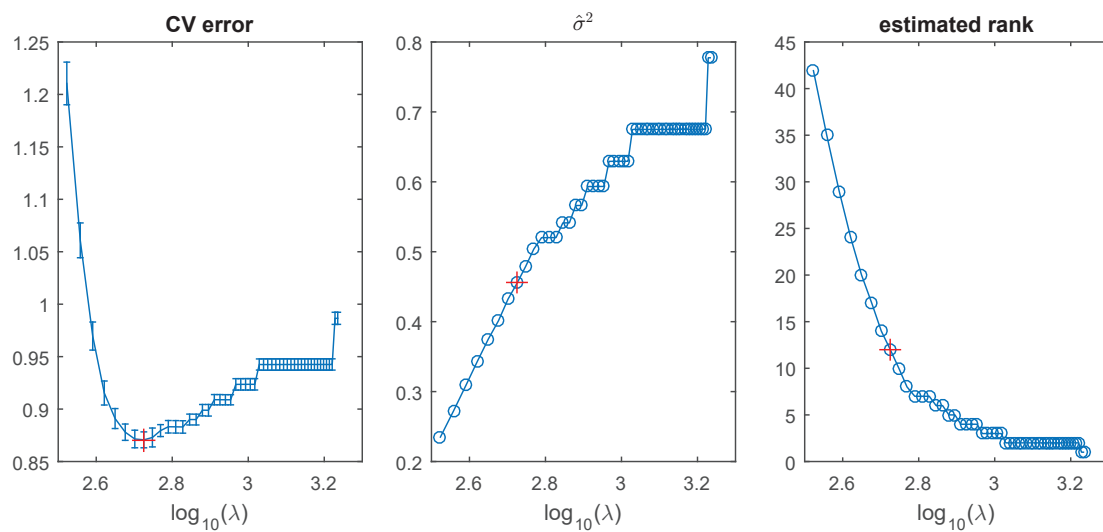


**Fig. S6** Model selection of the GSCA model with GDP penalty: CV error (left); estimated  $\hat{\sigma}^2$  (center); rank( $\hat{\mathbf{Z}}$ ) (right).

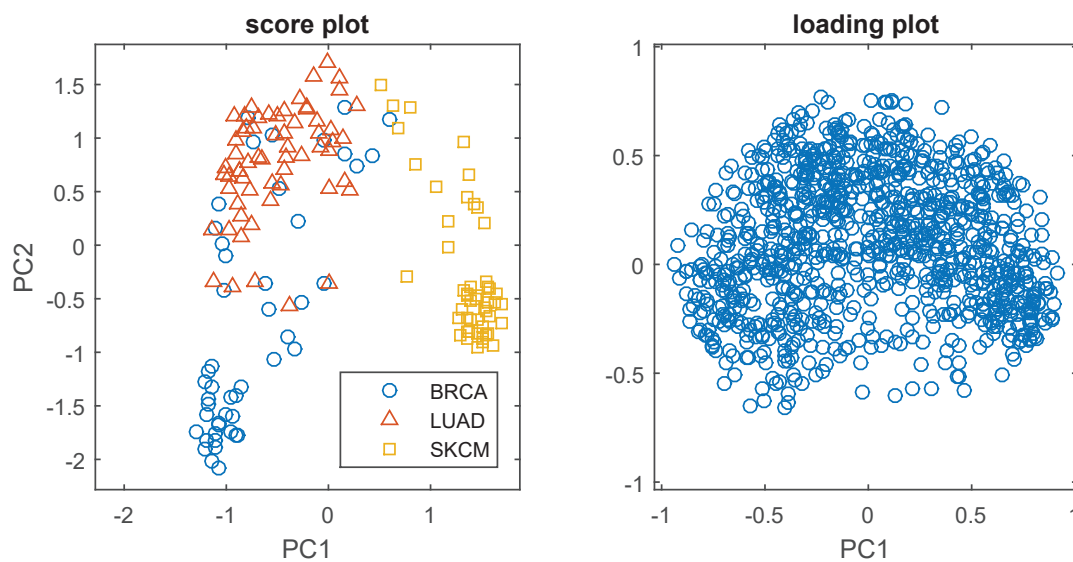


**Fig. S7** Score plot (left) and loading plot (right) derived from a PCA model on the gene expression data  $\mathbf{X}_2$ .  $\mathbf{X}_2$  are centered and scaled in the same as in the GSCA model. SVD algorithm is used to solve the PCA model.

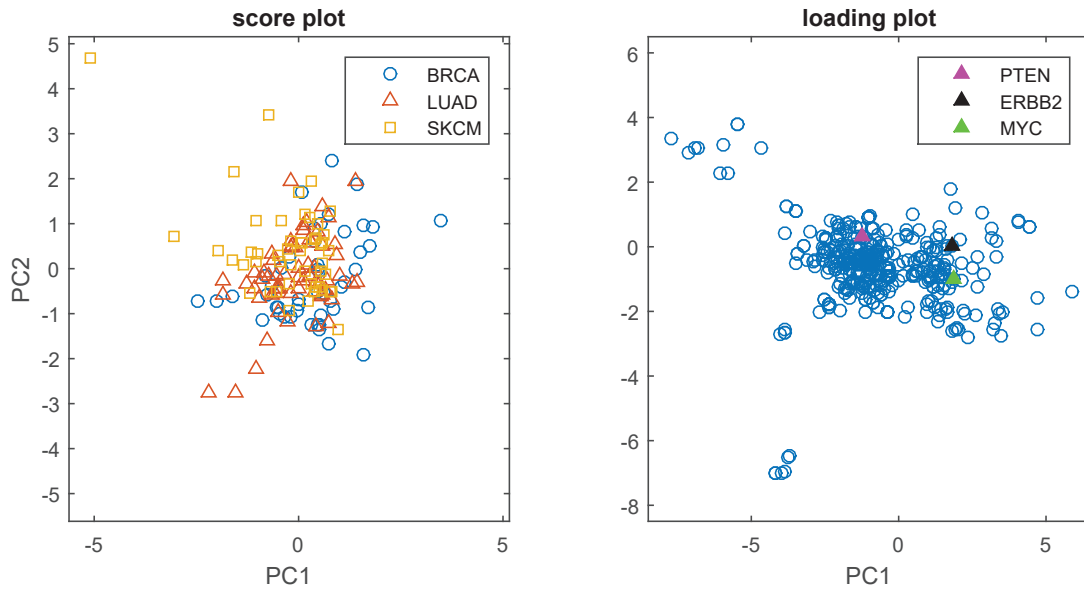


**Fig. S8** Score plot (left) and loading plot (right) are derived from a three components logistic PCA model on the CNA data  $\mathbf{X}_1$ .

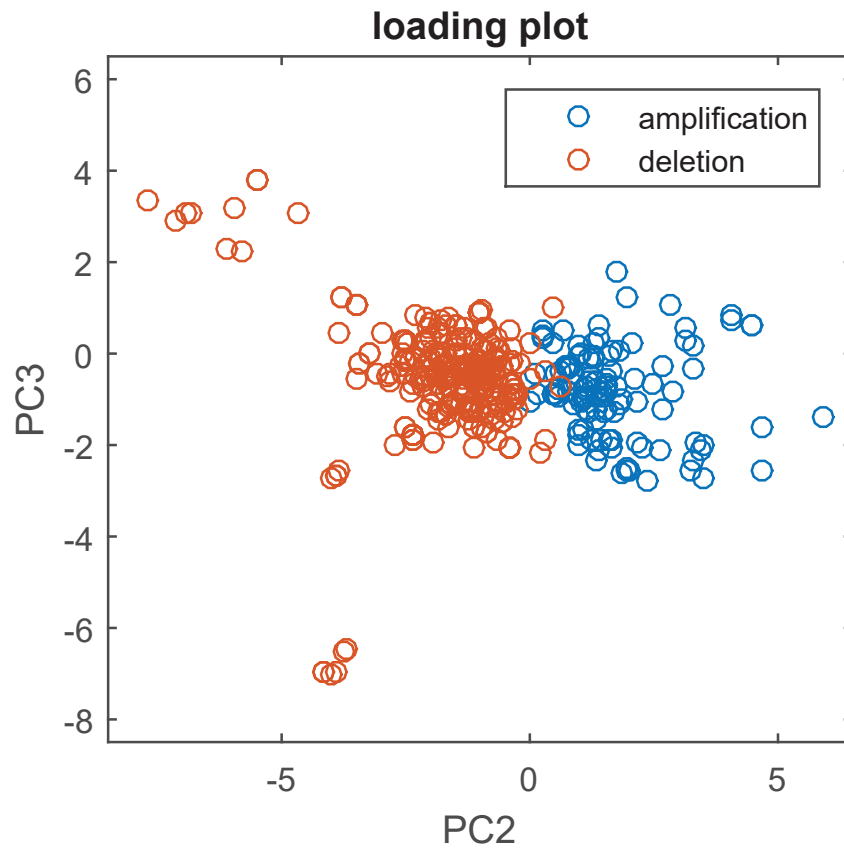


**Fig. S9** Loading plot derived from the three components logistic PCA model on the CNA data  $\mathbf{X}_1$ . The legend indicates the amplification or deletion of CNA feature.



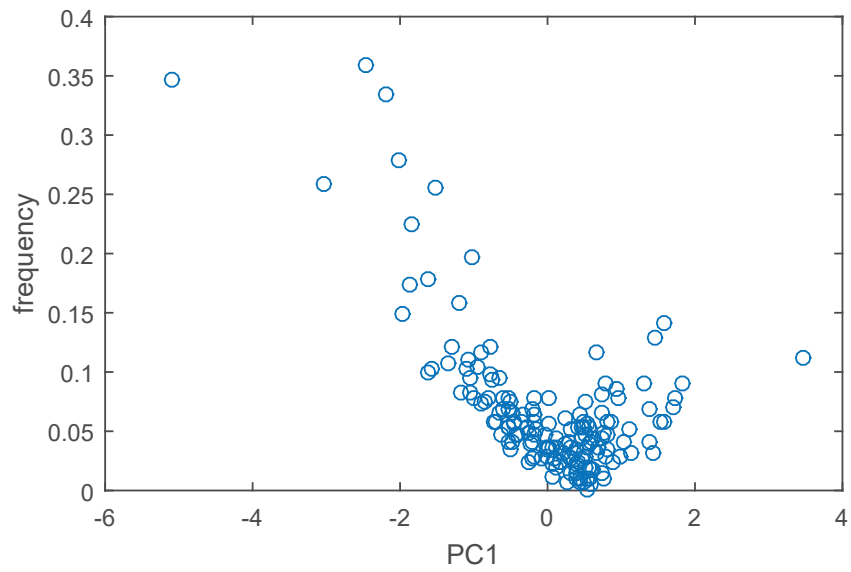


**Fig. S10** The relationship between PC1 scores and the frequency of aberrations of given samples derived from the three components logistic PCA model on the CNA data  $\mathbf{X}_1$ .

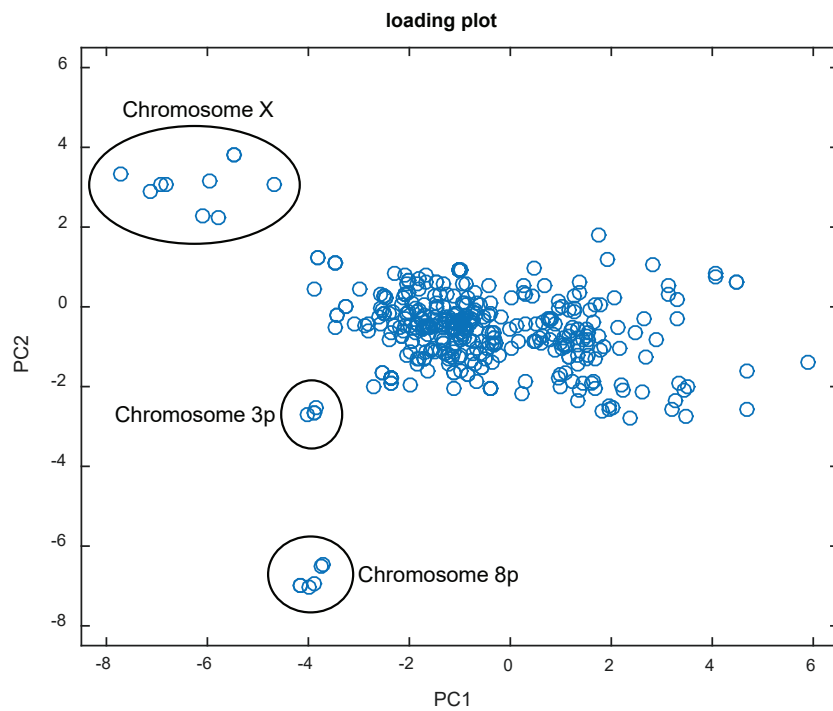


**Fig. S11** Loading plot derived from the three components logistic PCA model on the CNA data  $\mathbf{X}_1$ . The annotation indicates those features are in the same chromosome region.

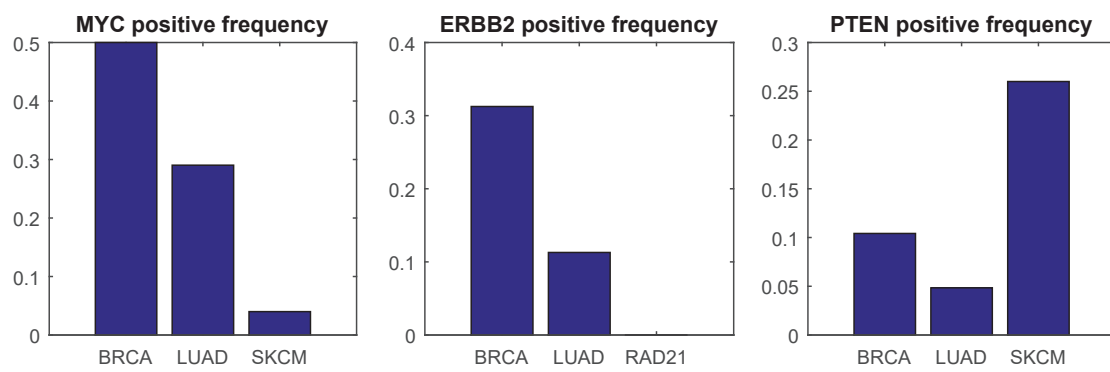


**Fig. S12** Positive frequencies of MYC, ERBB2 and PTEN features in three different cancer types.